AD-A055 420 AIR FORCE INST OF TECH WRIGHT-PATTERSON AFB OHIO SCH--ETC F/G 7/4
LIFETIME MEASUREMENTS USING FLUORESCENCE EMISSION.(U)
DEC 77 J J WHARTON

UNCLASSIFIED AFIT/GEP/PH/77-16 NL

1 OF 1
AD
A055 420

END
DATE FILMED
8-78
DDC

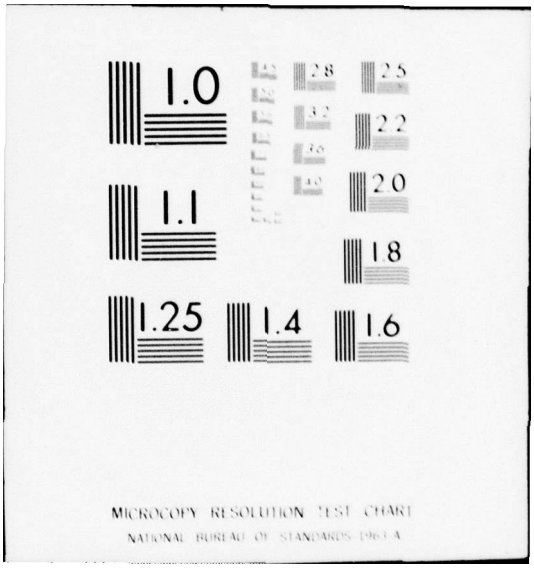
1.0
1.1
1.25
1.4
1.6
2.8
2.5
3.2
2.2
3.6
2.0
4.0
1.8
MICROCOPY RESOLUTION TEST CHART
NATIONAL BUREAU OF STANDARDS 1963-A

UNITED STATES AIR FORCE

AIR UNIVERSITY

AIR FORCE INSTITUTE OF TECHNOLOGY

Wright-Patterson Air Force Base, Ohio

GEP/PH/77-16

(1)

(6) LIFETIME MEASUREMENTS
USING FLUORESCENCE EMISSION.

(9) Master's thesis

THESIS

(14) AFIT/GEP/PH/77-16

(10) John J./Wharton, Jr./
Captain USAF

(11) Dec 77 (12) 72p.

Approved for public release; distribution unlimited

GEP/PH/77-16

LIFETIME MEASUREMENTS USING FLUORESCENCE EMISSION

THESIS

Presented to the Faculty of the School of Engineering

of the Air Force Institute of Technology

Air University

in Partial Fulfillment of the

Requirements for the Degree of

Master of Science

by

John J. Wharton Jr.

Captain USAF

Graduate Engineering Physics

December 1977

Preface

A thesis is much like an iceberg--only one-tenth of the work is ever seen. Hours of hard work and frustration are the price that must be paid for the knowledge and experience gained. However, at the end you find that that knowledge is a very rich reward.

My heartfelt thanks go to Paul Schreiber, my advisor, who taught me the patience and perseverance necessary for experimental work. Thanks also to Allen Hunter and the members of the AFIT Physics Department who encouraged me to take this experimental thesis topic.

This thesis was sponsored by the Air Force Aero Propulsion Laboratory. I would like to thank this organization for the equipment provided and for the help of its people. I would especially like to thank Dave Beard, Don Linder, and Sig Kizirnis for their help and expertise.

John J. Wharton

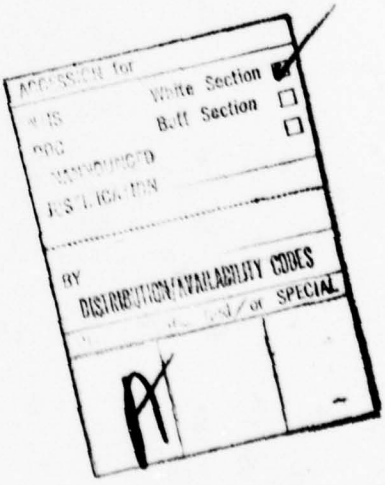

Contents

List of Figures

Abstract

Two experimental methods are developed for measuring fluorescence lifetimes on the order of ten nanoseconds. These data are necessary for measurements of species concentrations in combustion flames. The first method is based on counting photons within a fixed time interval, the position of which can be varied with respect to the excitation time of the sample. The second method uses a time to pulse height converter to measure the elapsed time between excitation of the sample and emission of a photon. The number of photons detected per laser pulse is reduced to one or less in order to obtain a valid statistical distribution. A tunable dye laser is used as the excitation source, and nitrogen dioxide is used as the test sample at pressures of 30 torr or less.

LIFETIME MEASUREMENTS

USING FLUORESCENCE EMISSION

I. Introduction

Background

For several years, the Air Force has been interested in developing non-perturbing diagnostic techniques to measure species concentrations and temperatures in combustion flames. This information could then be used to improve jet engine efficiencies and reduce the emission of pollutants into the atmosphere. Radiative diagnostic techniques are promising because they neither disturb the flame significantly nor introduce mechanical test probes into the exhaust.

Although optical radiation techniques have been used for over a century, the introduction of lasers in 1960 has expanded the use of these techniques. The organic-dye laser is an effective diagnostic tool because it can be tuned to any wavelength within a fixed wavelength band and because it can produce high peak powers in short pulses (Ref 17: 1-4).

Several optical diagnostic techniques have received close attention within the last five years. Among the most promising techniques are the following: (1) spontaneous Raman scattering, (2) coherent anti-Stokes Raman scattering (CARS), and (3) laser fluorescence (Ref 6:6-12). Each of these has strong and weak points with regard to their use in measuring species concentrations and temperatures.

Raman scattering is the inelastic scattering of light from atoms and molecules. Using the quantum theory of radiation, when a photon of

energy $h\nu$, where h is Planck's constant and ν is the frequency, undergoes an elastic collision with a molecule, the photon is scattered and this scattered light is of the same frequency as the incident light; this is termed Rayleigh scattering (Fig. 1a). However, if the collision is inelastic, energy is exchanged between the photon and the molecule. The scattered light is now of a different frequency and is termed Raman scattering. Scattered light of a frequency lower than the incident light is termed Stokes' radiation; if the frequency is higher, it is termed anti-Stokes' radiation (Ref 1:121-122). There are several advantages to using spontaneous Raman scattering in combustion diagnostics. First, visible wavelength lasers, which include tunable dye lasers, can be used. Additionally, the Raman spectrum is specific for a given molecule and is linearly proportional to the species number density. The major disadvantage of spontaneous Raman scattering is that the signal is very weak resulting in a very low signal to noise ratio (Ref 6:6-8).

Coherent anti-Stokes Raman scattering (CARS) is a non-linear optical process. Two laser sources, with frequencies ω_1 and ω_2, are selected such that $\omega_1 - \omega_2$ is tuned to a molecular vibrational resonance. The sample emits an intense collimated anti-Stokes beam at the frequency $\omega_3 = 2\omega_1 - \omega_2$ (Fig. 1b). Thus, one of the major advantages of CARS is that the light is collimated and more easily collected. Another advantage is that the CARS signal is much more intense than the spontaneous Raman scattering. Disadvantages to CARS are that two laser sources are required and the system is very sensitive to optical alignment (Ref 6:12).

Fluorescence is the emission of light resulting from the decay of a molecule from an excited electronic state (Fig. 1c). The molecule is

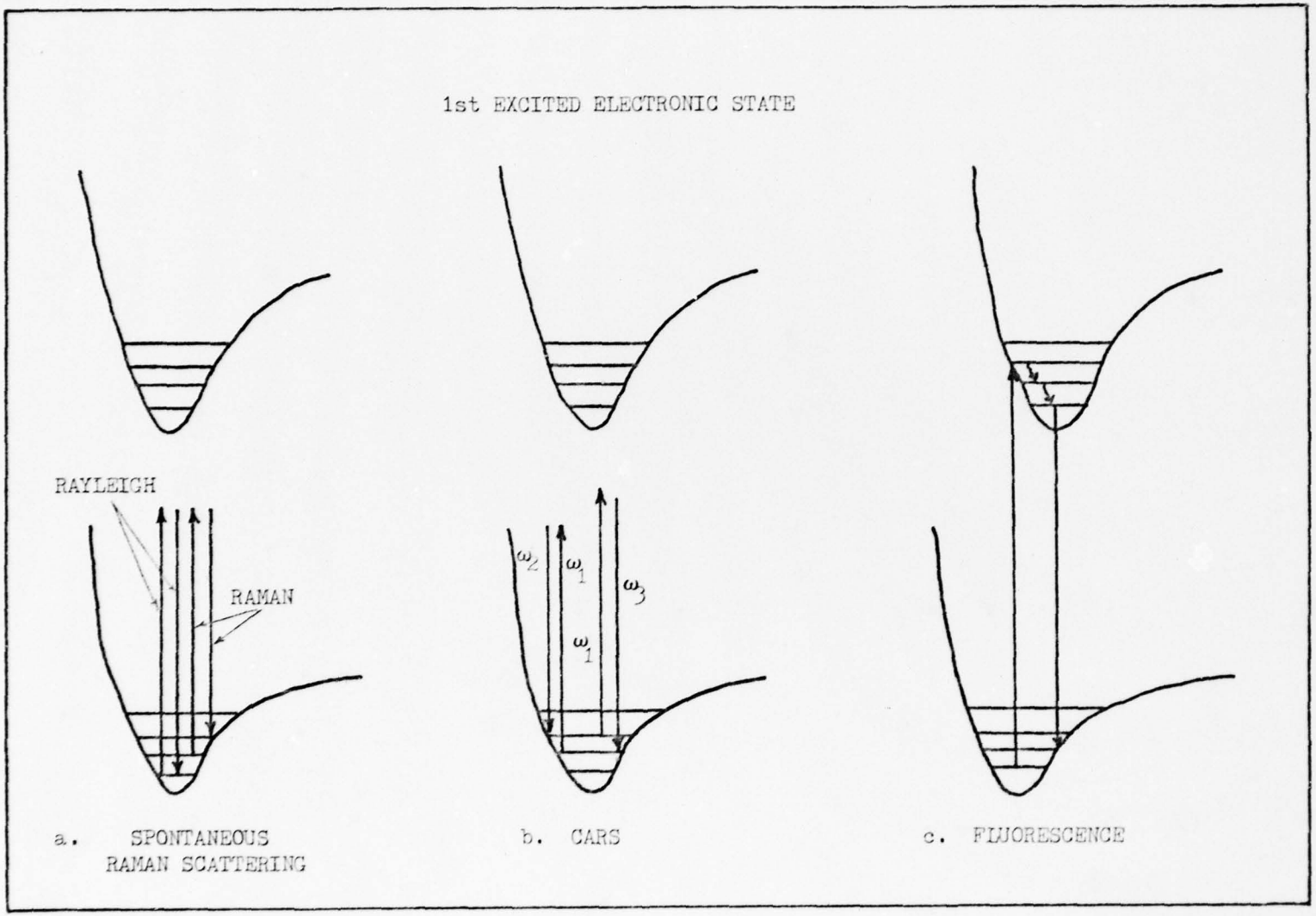

Fig. 1. Optical Diagnostic Techniques

normally excited through an inelastic collision with a photon of energy hν. After a lifetime characteristic of the excited state, the molecule can relax to the ground state by the spontaneous emission of a photon. This characteristic radiative lifetime can vary between 10^{-10} and 10^{+1} sec (Ref 6:8). The emitted fluorescence can be shifted in frequency from the frequency of the incident light or can be of the same frequency, termed resonance fluorescence. Although Raman scattering and fluorescence are both inelastic scattering processes, they are different since the exciting radiation for fluorescence must match the energy difference between the ground state and the excited state of the molecule.

There are other mechanisms that can compete with fluorescence in the loss of energy from the excited state of the molecule. Among these are dissociation, collisional deactivation, and intramolecular energy transfer. These processes are collectively called quenching and may dominate fluorescence. Such is often the case in combustion flames where many species are present to contribute to quenching. It should be possible to calculate the effect of the quenching theoretically if the concentrations of all species are known and if the collisional cross sections are known. The temperature must also be known because the rate of these processes depends on the temperature. Such a detailed knowledge of the combustion flame is usually not possible. The major advantage of fluorescence is that the fluorescence signal is usually much stronger than the spontaneous Raman scattering or CARS signal for the same stimulus. Thus, the signal to noise ratio is much improved. Also, the fluorescence signal is linearly dependent on species concentration.

There are four requirements that must be met if fluorescence is to be used for measurements of species concentration in combustion flames. First, the molecule of interest must have a known emission spectrum. Second, the molecule must have an absorption wavelength within the range of dyes available for the dye laser, assuming a dye laser is used. Third, the radiative lifetime must be known since the strength of the fluorescence signal is proportional to this decay rate. Fourth, if quenching mechanisms are present, their effect on the decay rate must be taken into account. It has been suggested that the following molecules, which are present in combustion flames, may be analyzed using fluorescence techniques: C_2, CH, CN, NH, NO, OH, C_6H_6, $C_{10}H_8$, $C_{14}H_{10}$, CH_2O, NO_2, and SO_2 (Ref 6:32).

Radiative Lifetime Measurements

To determine the radiative lifetime, which is required for the fluorescence technique, one of two conventional techniques has been used. The first technique consists of measuring the state population density and the volumetric emission coefficient. The radiative lifetime is then calculated directly by using the relation

$$\tau_{nm} = \frac{N_n \, h \, \nu_{nm}}{4 \pi E_{nm}} \qquad (1)$$

where τ_{nm} = the radiative lifetime

N_n = the state population density

E_{nm} = the volumetric emission coefficient

ν_{nm} = the transition frequency

h = Planck's constant (6.626×10^{-34} joule-sec)

The second technique consists of measuring the absorption coefficient and then calculating the radiative lifetime from the integrated absorption coefficient. The absorption coefficient is found using Beer's Law:

$$I(\nu) = I_o(\nu) \exp(-\alpha(\nu) L) \tag{2}$$

where $I(\nu)$ = the measured intensity (frequency dependent)

$I_o(\nu)$ = the initial intensity (frequency dependent)

$\alpha(\nu)$ = the absorption coefficient (frequency dependent)

L = the sample length

The stimulated emission coefficient (Einstein B_{nm} coefficient) is then found using the relation

$$B_{nm} = \alpha / [N_n h \nu_{nm}] \tag{3}$$

where α is the integrated absorption coefficient. The spontaneous emission coefficient (Einstein A coefficient), which is the inverse of the radiative lifetime τ, is related to the stimulated emission coefficient by

$$A = \frac{8 \pi h \nu_{nm}^3}{c^3} B_{nm} \tag{4}$$

where c is the speed of light.

However, both of these techniques require a detailed knowledge of the state populations of the gas. That is, two measurements are required to determine τ_{nm}. It is possible, however, to measure the radiative lifetime directly. Such a method may also be used to measure, rather than calculate, the effect of quenching corrections to the decay rate.

Purpose

The purpose of this thesis effort is to develop a method to directly measure radiative lifetimes based upon laser-induced fluorescence. This method must be capable of measuring lifetimes on the order of 10 nsec, as are expected in combustion flames. A tunable dye laser is used to promote a molecule to an excited state. The probability of emission of a photon after time t is proportional to exp $(-t/\tau)$. If the elapsed time t between excitation and photon emission is measured a statistically large number of times, then a plot of the natural logarithm of the frequency of the emission time t versus the time t will yield the lifetime τ.

Scope

The thesis effort is limited to developing an experimental apparatus to measure the elapsed time between excitation and photon emission in order to find the lifetime τ. A gas sample having a previously measured τ will be used as a standard for evaluating the experimental technique.

Nitrogen Dioxide

Because nitrogen dioxide (NO_2) is a major constituent in combustion flames and has absorption bands in the visible range of the spectrum, this gas is chosen as the gas sample to be used. In recent years NO_2 has received considerable attention. Not only is it present in combustion flames, but it is also an important component of the polluted atmosphere (Ref 20:1418). Another factor is that NO_2 has a much longer lifetime than that calculated using the integrated absorption coefficient (Ref 5, Ref 21:3457). Neuberger and Duncan have measured a mean lifetime

of fluorescence of 44.5 μsec (Ref 13:1694). Keyser, Kaufman and Zipf have measured radiative lifetimes on the order of 55 μsec (Ref 12:524), and Donnelly and Kaufman report lifetimes of about 200 μsec (Ref 4:4100).

The absorption spectrum of NO_2 has been recorded (Ref 14:230, Ref 9:507,602); however it has defied detailed analysis because of the high density of lines which show no obvious regularity (Ref 18:4977). Some transitions have been identified, and it has been determined that the $^2B_1$ state is the first excited state for vertical excitation (Ref 7: 1624, Ref 19:167). Information on potential energy surfaces has been presented by Gillispie, et al (Ref 8) and Jackels and Davidson (Ref 10, Ref 11).

From an experimental point of view, NO_2 is a difficult gas to work with. It is a toxic, corrosive gas. Additionally, the gas exists as a mixture of both NO_2 and N_2O_4 with the concentration varying by temperature and pressure.

The theory of rate equations and photon counting are discussed in Chapter II. The equipment used is described in Chapter III followed by a discussion of the procedures in Chapter IV. Chapter V gives a summary of results, and Chapter VI gives a list of conclusions and recommendations.

II. Theory

The physical theory which supports the experimental methods is discussed in this section. The rate equations for state population densities are developed, followed by a discussion of transition probabilities. Next, photon counting methods are discussed. Finally, an estimate is made of the fluorescence strength and counting rate that are expected.

Rate Equations

To determine the rate at which energy is transferred between energy states of any species, it is useful to develop a two-level model. Such a model is shown in Fig. 2.

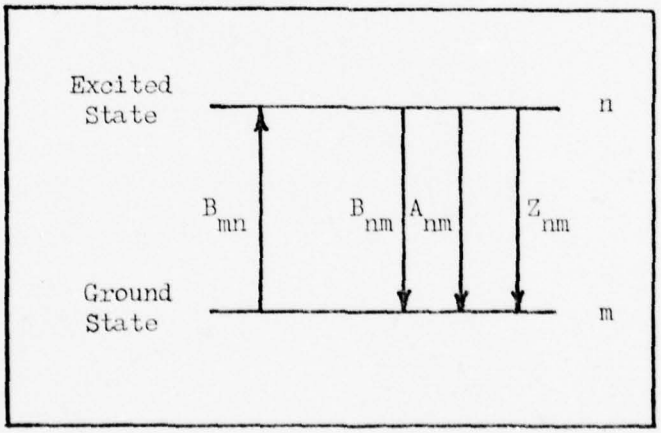

Fig. 2. Two-level Model

The rate equation for this model is then developed term by term.

Excitation of a molecule is written as an absorption term dependent on the Einstein B_{mn} coefficient. This absorption term is written

$B_{mn} I N_m$ where I is the intensity of the laser beam and N_m is the ground state population density. In similar manner, energy can be transferred from the excited state to the ground state through stimulated emission. The rate at which this occurs is given by $B_{nm} I N_n$ where N_n is the excited state population density. The two Einstein B coefficients are related by the equation

$$B_{nm} g_n = B_{mn} g_m \tag{5}$$

where g_i is the degeneracy of any level i.

The spontaneous emission of photons from the excited state occurs at the rate $A_{nm} N_n$ where A_{nm} is the Einstein A coefficient. Collisional deactivation occurs at a rate $Z_{nm} N_n N_m$ where Z_{nm} is some collisional rate constant. If other species are present and contribute to collisional deactivation, they can be represented by an additional term $Z_{nl} N_n N_l$ where N_l is the density of the additional species. Self-collisions are represented by the term $Z_{nn} N_n^2$. There may also be a loss of particles through diffusion of particles outside the region of observation. This occurs at a rate $D_f \nabla^2 N_n$, where D_f is the diffusion coefficient (Ref 2: 25-28).

Thus, the rate equation for the excited state may be written

$$dN_n/dt = B_{mn} I N_m - A_{nm} N_n - B_{nm} I N_n - Z_{nm} N_n N_m - Z_{nl} N_n N_l - Z_{nn} N_n^2 + D_f \nabla^2 N_n \tag{6}$$

After the laser pulse, the first and third terms of this equation are zero. If diffusion is assumed to be small, the last term can be neglected. This can be shown to be the case for NO_2 at pressures of interest. Also Z_{nn} is small, and that term can be neglected. If the signal is small, then N_m and N_l are constants. This applies for the case far

from saturation. The collisional terms can then be represented by the collective quenching term $Q\ N_n$, where Q is a constant. The rate equation then reduces to

$$dN_n/dt = -\ (\ A_{nm} + Q)\ N_n \tag{7}$$

The solution to this equation is

$$N_n = N_o \exp\left[-\ (\ A_{nm} + Q)\ t\right] \tag{8}$$

where N_o is the excited state population density at the end of the laser pulse, time t = 0. The characteristic lifetime τ is given by

$$\tau = (\ A_{nm} + Q\ )^{-1} \tag{9}$$

If the spontaneous emission dominates collisional quenching, then τ is the radiative lifetime.

If the quenching Q of Eq (9) is linearly dependent on the pressure, then the equation can be written in the form

$$\tau^{-1} = A_{nm} + q\ P \tag{10}$$

where q is the quenching constant and P is the pressure. A plot of the inverse of the lifetime versus the pressure will yield a straight line, such as is shown in Fig. 3 (Ref 13:1694). This line will yield q, and extrapolation to zero pressure will yield the radiative lifetime.

It is also useful to examine the near saturation case when the intensity of the laser is large. For this case N_m is not a constant. It will be assumed that the additional species N_1 remains constant at a fixed temperature and pressure. Since $N_m + N_n = N$ (a constant), the rate equation becomes

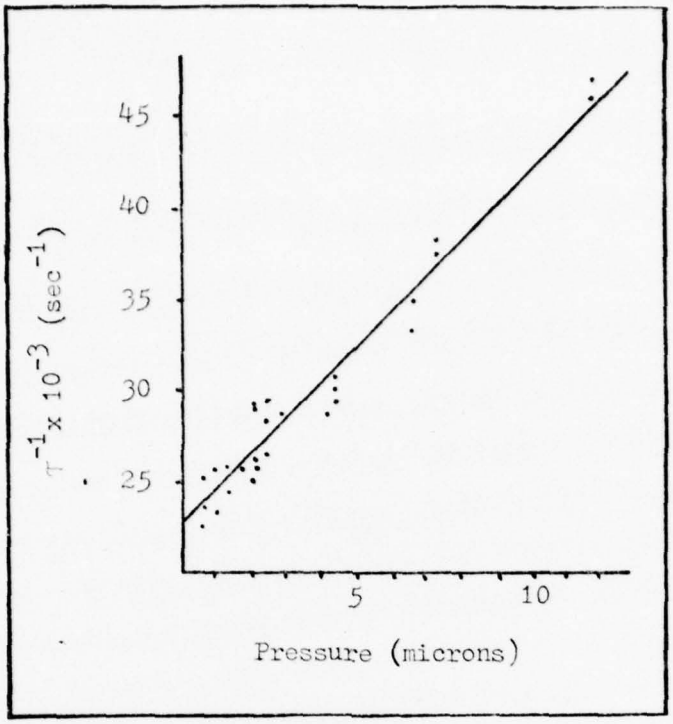

Fig. 3. Reciprocal of Lifetime as a Function of Pressure (Ref 13:1694)

$$dN_n/dt = - A_{nm}N_n - Z_{nm}N_n (N - N_n) - Z_{nl}N_nN_l \tag{11}$$

This can be rewritten as

$$dN_n/dt = - (A_{nm} + Z_{nm}N + Z_{nl}N_l) N_n + Z_{nm}N_n^2 \tag{12}$$

The solution to this equation is

$$N_n(t) = \frac{\gamma \exp(-\gamma t)}{Z_{nm} \exp(-\gamma t) - (Z_{nm}N_o - \gamma)/ N_o} \tag{13}$$

where $\gamma = A_{nm} + Z_{nm}N + Z_{nl}N_l$. A detailed examination of the case of saturation has been made by Piepmeier (Ref 15:435-438).

Both of these two-level models can be used for resonance fluorescence. However, when excitation occurs at one wavelength and radiative emission is observed at another wavelength, non-resonance fluorescence

is observed, and a three-level model must be used. A three-level model is shown in Fig. 4 and again neglects diffusion and self-collisions.

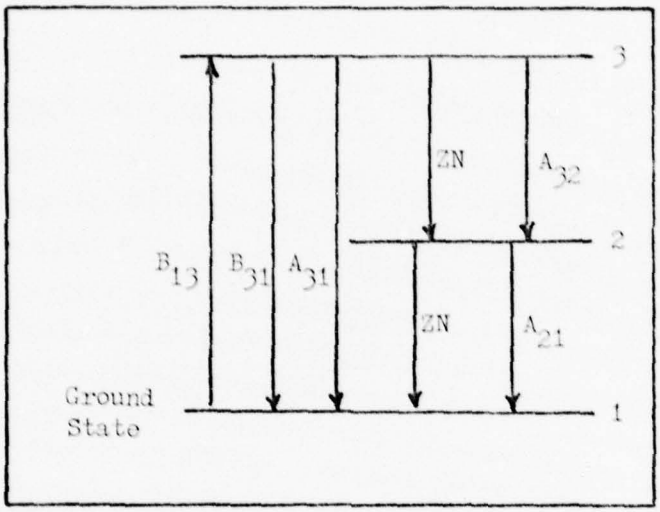

Fig. 4. Three-level Model

An assumption that the collisional cross-section Z_{21} is very small, and an assumption that the other collisional cross sections are the same and independent of collision partners, yields the following set of equations for after the laser pulse:

$$dN_3/dt = - A_{31}N_3 - A_{32}N_3 - Z\,N_3N \tag{14}$$

$$dN_2/dt = A_{32}N_3 + Z\,N_3N - A_{21}N_2 - Z\,N_2N \tag{15}$$

$$dN_1/dt = A_{31}N_3 + A_{21}N_2 + Z\,N_2N \tag{16}$$

where N is the total number of molecules, and is a constant. The solution to Eq (14) is

$$N_3 = N_{3_o} \exp\left[-(A_{31} + A_{32} + Z\,N)\,t\right] \tag{17}$$

Eq (15) is then of the form

$$dN_2/dt + (A_{21} + Z\ N)\ N_2 = f(t) \tag{18}$$

Thus, the solution to Eq (15) is

$$N_2 = \frac{N_{3o}\ (A_{32} + Z\ N)}{A_{21} - A_{31} - A_{32}}\left[\exp\left[- (A_{31} + A_{32} + ZN)\ t\right] - \exp\left[- (A_{21} + ZN)\ t\right]\right] \tag{19}$$

If it is assumed that the radiative decay from level 2 to level 1 dominates the collisions, and further assumed that collisions dominate the depopulation of level 3, then $A_{21} > ZN \gg A_{32}, A_{31}$. Eq (19) becomes

$$N_2 = \frac{Z\ N\ N_{3o}}{A_{21}}\left[1 - \exp\ (-A_{21}\ t)\right]\ \exp\ (-Z\ N\ t) \tag{20}$$

This equation shows that when collisional deactivation quickly populates level 2, the fluorescence observed from level 2 is a measurement of the collisional deactivation rate. If the fluorescence is observed from level 3 to level 2, then Eq (17) is the form of the exponential decay observed.

An additional set of rate equations can be written for the case where collisional deactivation depopulates level 3 and a different collisional rate applies to deactivation between levels 2 and 1. The rate equations become

$$dN_3/dt = - Z\ N_3 N \tag{21}$$

$$dN_2/dt = Z\ N_3 N - A_{21} N_2 - Q\ N_2 \tag{22}$$

$$dN_1/dt = A_{21} N_2 + Q\ N_2 \tag{23}$$

In these equations, Q is the quenching constant between levels 1 and 2. Solving the equations for N_2 and N_3 yields the following:

$$N_2 = N_{3_o} \left[\exp\left[- (A_{21} + Q)\ t \right] - \exp\ (-\ Z\ N\ t) \right] \qquad (24)$$

and

$$N_3 = N_{3_o}\ \exp\ (-\ Z\ N\ t) \qquad (25)$$

Thus for fluorescence from level 2 to level 1, Eq (24) gives the form of the decay.

Transition Probabilities

As can be seen from Eqs (8), (17), (20), and (24), the fluorescence signal observed will depend on the number of molecules initially excited by the laser pulse. As previously noted, the energy of the exciting radiation must match the energy difference of the ground state and the excited state. Additionally, the strength of the absorption will depend on the number of molecules in the ground state. Since there are many vibrational states for each electronic level, there are many possible transitions. However, according to the Franck-Condon principle, electronic transitions occur so rapidly that the internuclear distance of the molecule does not change during the transition (Ref 1:208). Thus, electronic transitions must occur vertically on potential energy curves plotted versus internuclear distance. This is shown schematically in Fig. 5. Since most of the molecules are in the lowest vibrational state of the ground electronic state, the transition labeled (0,3) in Fig. 5 is the strongest. It should be noted that the most probable internuclear distance for the lowest vibrational state is at the center; for higher vibrational states, it is at the edges on the curve. Therefore, a transition occurs between the v = 0 vibrational level of the upper electronic

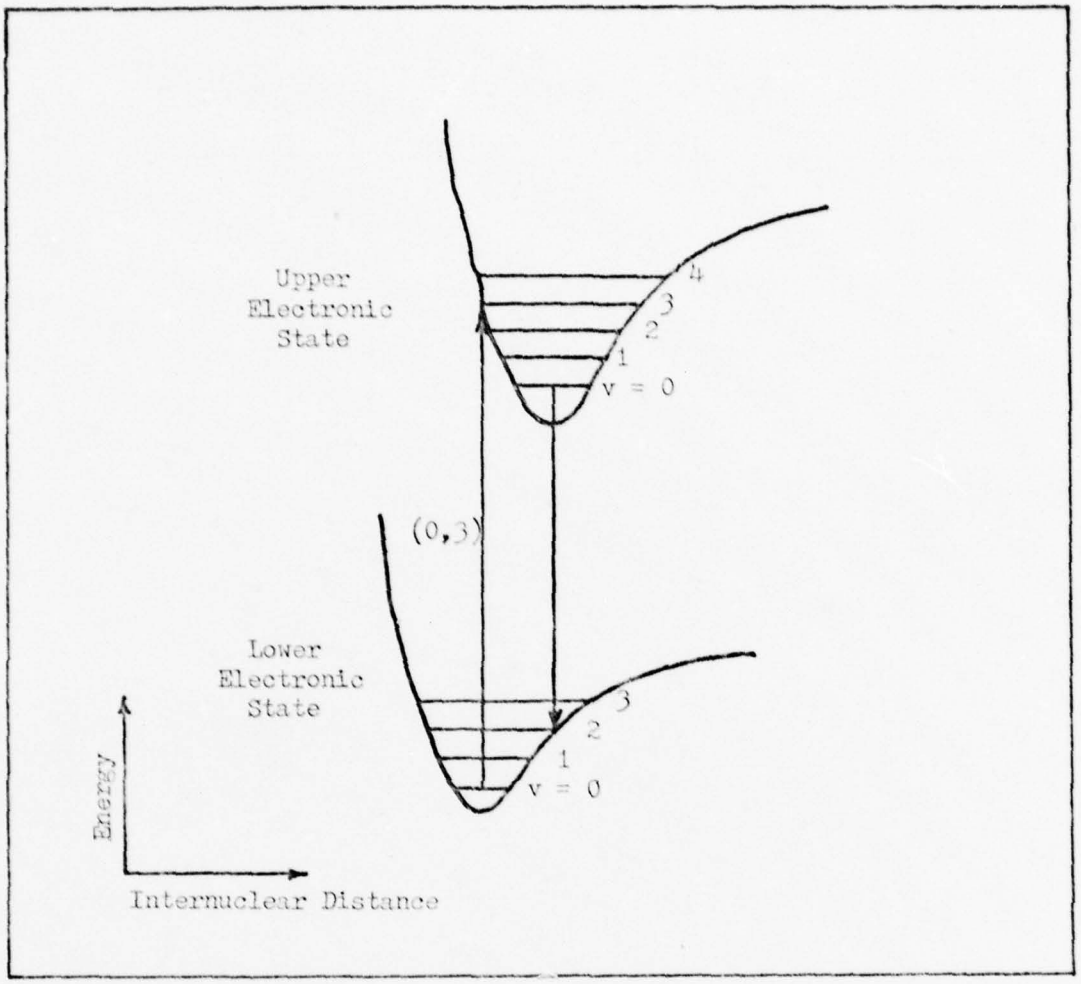

Fig. 5. Franck-Condon Principle

state and the v = 2 vibrational level of the lower electronic state. These become important considerations for molecules where the upper electronic potential energy curve is shifted from the lower electronic potential curve. Some of the potential energy curves for NO_2 are shown in Fig. 6 (Ref 8:3436), where the potential energy is plotted as a function of bond angle. The principle of vertical transitions applies; thus, excitation to the first excited electronic state requires 2.8 eV or a wavelength of 4409 Å.

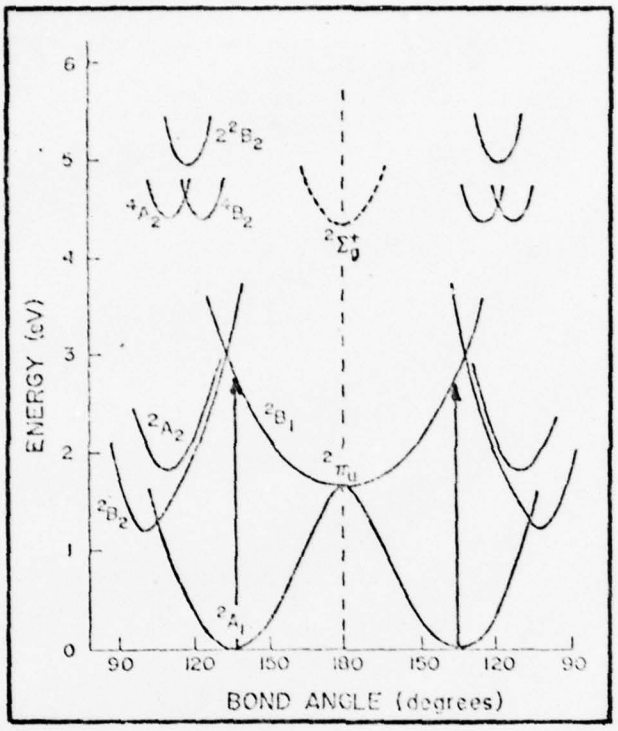

Fig. 6. NO_2 Potential Energy Curves (Ref 8:3436)

Photon Counting

Once the fluorescence wavelength has been selected, a method must be devised to detect the rate at which the photons are emitted; two methods are proposed. The first method consists of counting the number of photons detected during a fixed time interval τ. This fixed interval is then moved to varying times after the laser pulse as illustrated in Fig. 7. To show that this determines the decay lifetime τ, the probability of getting counts must be determined.

The probability of counting photons in some small interval Δt at time t is given by

$$P_{\Delta t} = P_c \, N(t) \, A_{nm} \, \Delta t \qquad (26)$$

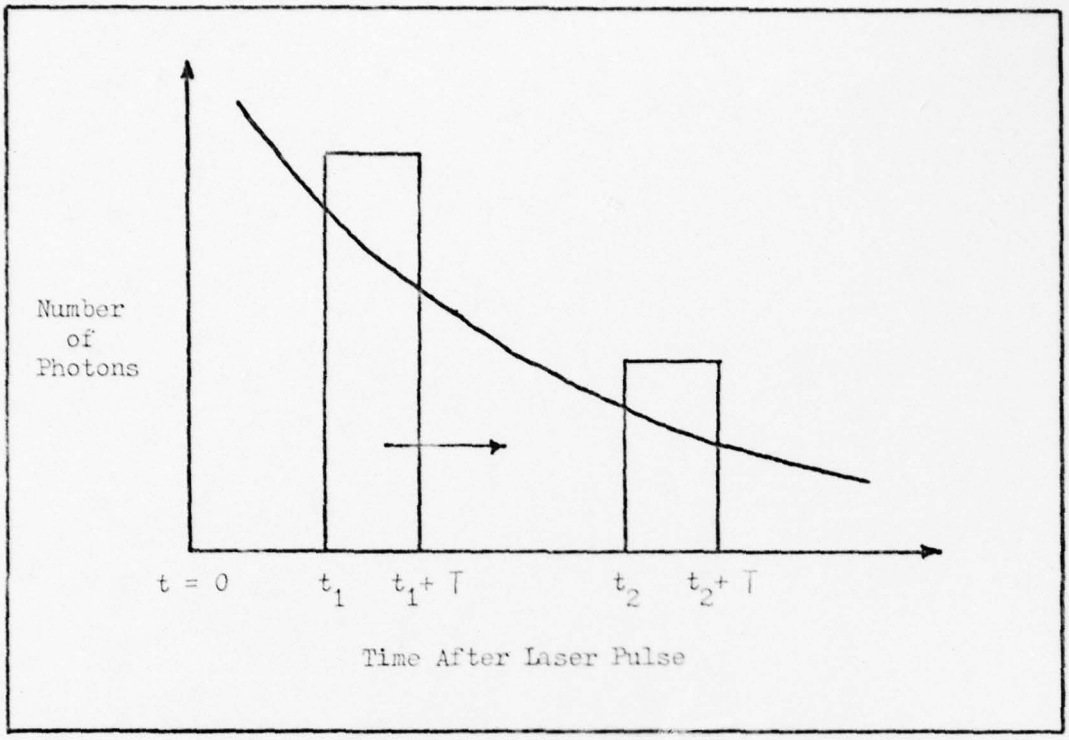

Fig. 7. Photon Counting Method

where P_c is a collection probability constant, $N(t)$ is the number of molecules in the excited state at time t, and A_{nm} is the transition probability. The probability of getting photons in the interval t to $t + \tau$ is

$$P_{\Delta t}(t) = \int_t^{t+\tau} P_c \, N(t) \, A_{nm} \, dt \tag{27}$$

If $N(t)$ is given by Eq (8), and quenching can be neglected, then Eq (27) becomes

$$P(t) = \int_t^{t+\tau} A_{nm} \, P_c \, N_o \exp\left(-A_{nm} t\right) dt \tag{28}$$

which reduces to

$$P(t) = P_c \, N_o \left[\exp\left(-A_{nm} t\right)\right]\left[1 - \exp\left(-A_{nm} \tau\right)\right] \tag{29}$$

Since the last term of Eq (29) is just a constant, the probability of counting photons is an exponential determined by the decay rate. If quenching contributes to the decay rate, as given by Eq (8), then Eq (29) becomes

$$P(t) = C \exp\left[-(A_{nm} + Q)\, t\right] \tag{30}$$

where

$$C = \frac{P_c\, N_o\, A_{nm}}{A_{nm} + Q}\left[1 - \exp\left(-A_{nm}\tau\right)\right] \tag{31}$$

The decay rate measured is then the combined radiative and quenching terms. To avoid detection of two photons at once, the counting rate is kept to less than one photon per laser pulse.

The other method of measuring the lifetime consists of measuring the time elapsed between the end of the laser pulse and the emission of a photon. Since the timing equipment detects the first photon, it is necessary to determine the probability of getting any photon in the time interval t to t + Δt.

Let q = the probability that a molecule will not decay prior to time t

p = the probability that a molecule will decay in the next time interval, t to t + Δt

P_c = the probability that a photon will be detected

N_o = the initial number of excited molecules at time t = 0

The probability of detecting a photon in the interval t to t + Δt, for N_o = 1 is then

$$P = q\, p\, P_c \tag{32}$$

For N_o = 2, either both molecules are still excited at time t or one is still excited and the other molecule has decayed but was not detected.

The probability of detecting a photon in the interval t to t + Δt is then

$$P = 2\, q^2 p\, P_c + 2\, q\, (1 - q)(1 - P_c)\, p\, P_c \qquad (33)$$

For $N_o = 3$, three molecules can be excited at time t, or two molecules can be excited at time t with one molecule decayed but the photon not detected, or one molecule can be excited at time t with two molecules decayed and neither detected. The probability of detecting a photon in the interval t to t + Δt is

$$P = 3\, q^3 p\, P_c + 6\, q^2 p\, P_c (1 - q)(1 - P_c) + 3\, q\, p\, P_c (1 - q)^2 (1 - P_c)^2 \qquad (34)$$

For the general case of N_o excited atoms, the probability of detecting a photon in the interval t to t + Δt is by induction

$$P = p\, P_c \left[\sum_{m=1}^{N_o} \frac{m\, N_o!}{m!\, (N_o - m)!}\, q^m \left[1 - q\right]^{(N_o - m)} \left[1 - P_c\right]^{(N_o - m)} \right] \qquad (35)$$

This can be written in the form

$$P = p\, P_c\, N_o\, q \left[1 - P_c (1 - q)\right]^{(N_o - 1)} \qquad (36)$$

Substituting $p = \Delta t/\tau$ and $q = \exp(-t/\tau)$, Eq (36) becomes

$$P = P_c N_o \Delta t\, \tau^{-1} \exp(-t/\tau) \left[1 - P_c \left[1 - \exp(-t/\tau) \right] \right]^{(N_o - 1)} \qquad (37)$$

Note that for large N_o, $N_o - 1 \approx N_o$, and keeping only the first terms

$$P = P_c N_o\, \Delta t\, \tau^{-1} \left[\exp(-t/\tau) \right] \left[1 - N_o P_c \left[1 - \exp(-t/\tau) \right] \right] \qquad (38)$$

If the probability of detection of a photon is kept less than one per laser pulse, then $N_o P_c < 1$ and Eq (38) becomes

$$P = P_c N_o\, \Delta t\, \tau^{-1} \exp(-t/\tau) \qquad (39)$$

By the use of neutral density filters, the number of photons detected per laser pulse can be kept to one or less. The probability of detecting a photon at time t is then given by Eq (39) and has the form of exp $(-t/T)$. The error in these counting methods is controlled by Poisson statistics. The result is that the standard deviation in the number of counts which are measured is given by the square root of the number of counts (Ref 16:52-56).

Estimate of Fluorescence Counts

Having established the theory of fluorescence decay measurements, an order of magnitude estimate is made of the number of counts expected. This estimate depends on at least the following: (1) the pulse shape and power of the laser, (2) the absorption properties of the gas, (3) the emission intensity, (4) the collection efficiency of the lens and monochromator, (5) the quantum efficiency of the photomultiplier tube, and (6) the time interval examined by the detection electronics. An estimate of these factors is made for NO_2.

The absorption per unit length is given by

$$dI(x,\nu,t)/dx = - \alpha_i(\nu)\ I(x,\nu,t) \tag{40}$$

where I is the intensity and α_i is an absorption line as a function of frequency. Integrating over a cross-sectional area yields the power

$$dP(x,\nu,t)/dx = - \alpha_i(\nu)\ P(x,\nu,t) \tag{41}$$

Integration yields

$$P(x,\nu,t) = P_o(\nu,t)\ \exp[\ - \alpha_i(\nu)\ x\ ] \tag{42}$$

Assuming that $\alpha_i(\nu)$ is small, the equation becomes

$$P(x,\nu,t) \approx P_o(\nu,t)\left[1 - \alpha_i(\nu)\ x\right] \tag{43}$$

Integrating over frequency yields the total power at point x

$$P_T(x,t) = P_{TL} - x\int_0^\infty P_o(\nu,t)\ \alpha_i(\nu)\ d\nu \tag{44}$$

where P_{TL} is the total laser power.

Individual absorption lines are not observed, however, and a constant absorption α_T is assumed over the spectral width of the laser. Thus Eq (44) becomes

$$P_T(x,t) = P_{TL}\ (\ 1 - \alpha_T\ x\ ) \tag{45}$$

Thus the fractional power absorbed is

$$\Delta P/P_{TL} = \alpha_T\ x \tag{46}$$

Integration over time yields the energy. The energy absorbed in a length d is then

$$\Delta E = E\ \beta\ d\ /\ \ell \tag{47}$$

where β is the fraction of energy absorbed after some length ℓ.

Based upon preliminary investigations, there is an intensity absorption of 20% for a sample length of 35 cm when using the dye Coumarin 440. This dye has a pulse energy of 800 microjoules at 4304 $\mathring{A}$, which is reduced to 400 microjoules because of optical elements prior to the gas sample. The length of gas viewed by the monochromator is 1 mm. Using these numbers in Eq (47), the energy absorbed is 2.3×10^{-7} joules. Assuming that all of this energy is used to excite molecules, the number of molecules in the excited state after one laser pulse is given by $\Delta E\ /\ h\ \nu$; this is 5×10^{11} molecules. The absorption measurement was

made at a pressure of 20 torr; for 1 torr, the number of molecules excited would be 2.5×10^{10}. If all of the molecules deactivate radiatively, then 2.5×10^{10} photons would be emitted in a solid angle of 4π. The lens, which focuses the fluorescence onto the entrance slit of the monochromator and approximately fills the grating, captures a solid angle given by

$$\Omega = \pi r^2 / y^2 \tag{48}$$

where Ω is the solid angle, r is the radius of the lens, and y is the distance of the lens to the laser beam path. The lens has a radius of 1.27 cm and is 25.4 cm from the laser beam path. Thus, the number of photons entering the monochromator is 3×10^8.

Assuming that the monochromator delivers half of the photons to the photomultiplier tube, the number of photons at the photomultiplier tube is 1.5×10^8. The quantum efficiency for the photomultiplier, which has an S-20 response, is 20% at 4304 Å. Thus, the total number of photoelectrons originating at the photocathode of the photomultiplier tube is 3×10^7. The electronics only sample the first 500 nsec after the laser pulse, so if the lifetime is on the order of 100 μsec, Eq (39) yields a total count of 1.5×10^5. This is an upper bound estimate since there may be other possible losses. However, this calculation shows that the number of available counts is more than adequate and could be reduced through the use of neutral density filters.

III. Equipment

The equipment used for this experiment is divided into the following categories: (1) gas handling system, (2) laser, (3) optics, and (4) electronics. Each of these categories will be discussed separately. A photograph of the overall experimental setup is shown in Fig. 8.

Gas Handling System

A photograph of the gas handling system is shown in Fig. 9 and a schematic is given in Fig. 10. The sample of NO_2 comes from a Whitey lecture bottle of length 20 cm and diameter 5 cm. The tubing for the gas system is 1/4 inch and 1/2 inch stainless steel; Swagelok fittings are used. Valve 3, shown in Fig. 10, is a Whitey needle valve; all other valves are Nupro bellows valves. The gas enters a glass sample tube through a hole of 1 cm diameter. This sample tube is 35 cm long and has a diameter of 5 cm. A fluorescence port 7 cm long is located 21.5 cm from the end of the tube nearest the dye laser. The entrance window, exit window, and fluorescence window are made of quartz.

The sample tube is wrapped with Briskeat heat tape for sample heating. An insulative box 40 cm by 23 cm can be placed around the sample tube. This box has three ports for laser beam entry and exit and fluorescence viewing. An Assembly Products, Inc. temperature gauge, which uses an iron-constantine thermocouple, is mounted to the box to monitor the temperature; the maximum reading is 105°C.

The pressure within the sample tube is monitored using either an Ace Glass mercury McLeod gauge or a Container Service, Inc. Model VG 1000 thermocouple gauge, each capable of measuring pressures as low

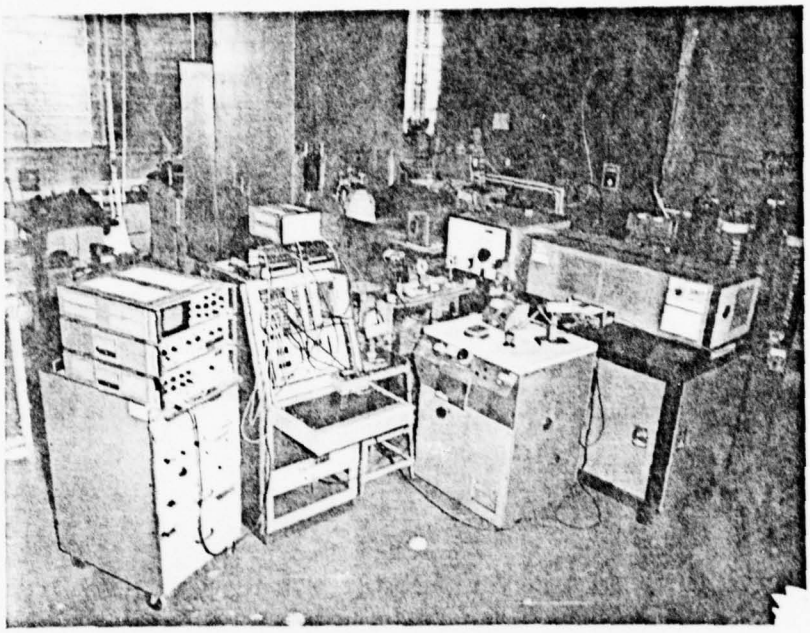

Fig. 8. Photograph of Experimental Setup

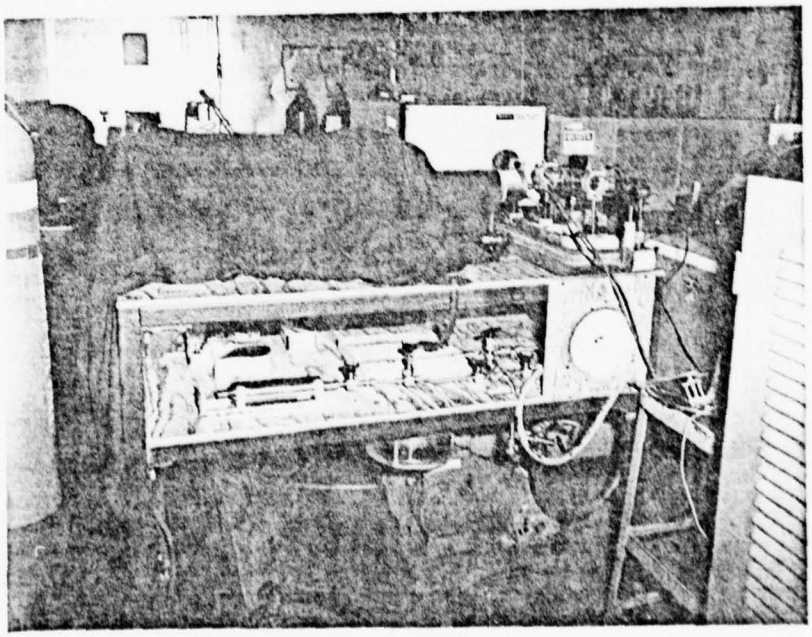

Fig. 9. Photograph of Gas Handling System

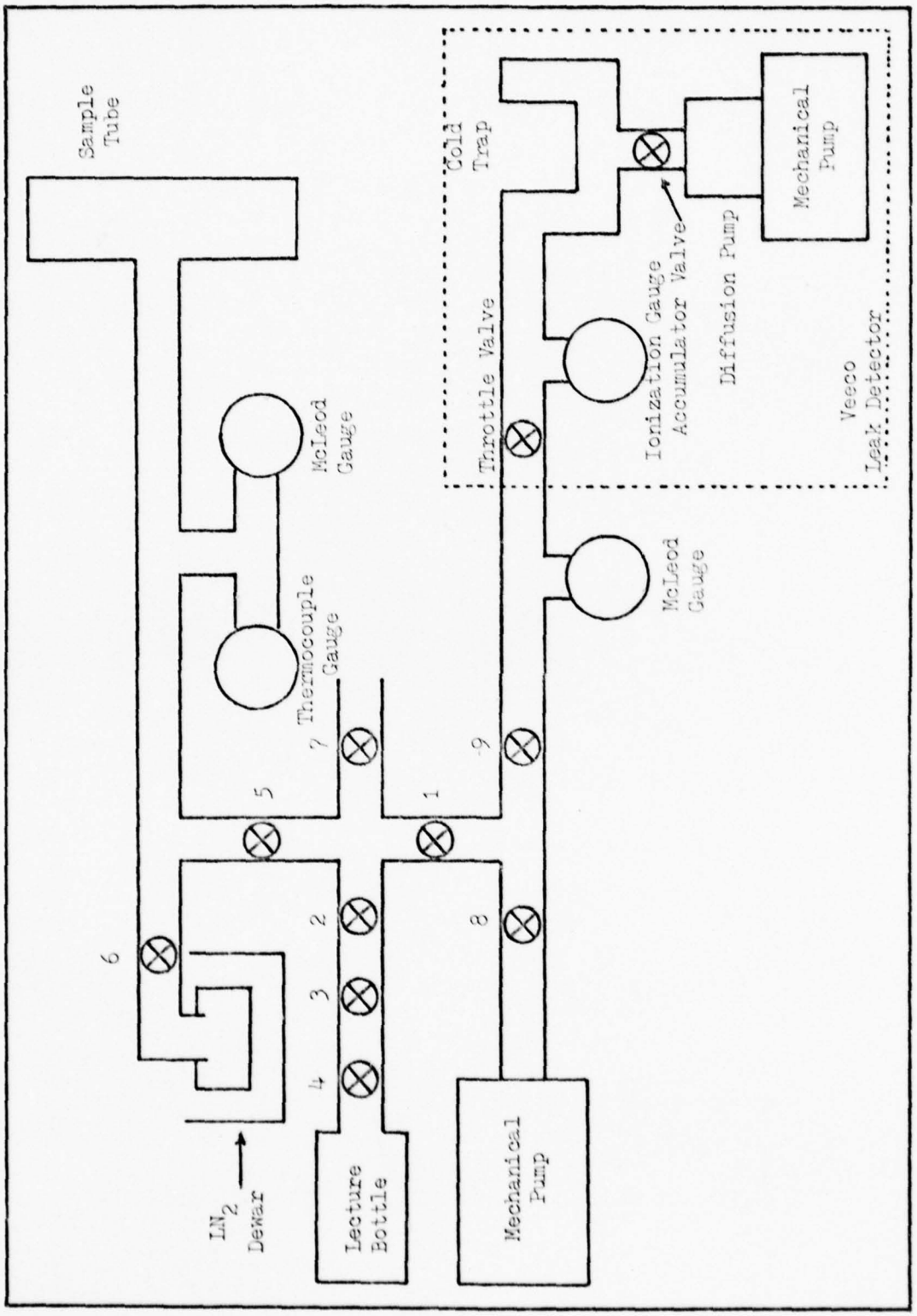

Fig. 10. Gas Handling System

as one millitorr, one micron. Since NO_2 is a toxic, corrosive material, the gas within the sample tube is removed by freezing out into a 20 cm long, 6 cm diameter metal bottle submerged in a liquid nitrogen (LN_2) Dewar. The system is initially pumped out using a Welch mechanical pump. Pressures as low as one micron can then be reached using the diffusing pump of a Veeco Model MS-9 leak detector. The pressure just prior to the leak detector is monitored using an additional Ace Glass mercury McLeod gauge.

Laser

A Molectron DL200 Tunable Dye Laser is used as an excitation source and is pumped by a Molectron UV1000 Nitrogen (N_2) Laser with a peak power of one megawatt at 3371 Å. The N_2 laser can be pulsed at 5, 10, 15, 20, 25, 30, 40, or 50 pulses per second with a pulse width of 3 to 10 nsec. This also determines the pulse rate of the dye laser, which can be tuned over the range 3600 Å to 7500 Å by the selection of various organic dyes. Four dyes were used during the course of the experiment, and a plot of their relative pulse energy versus wavelength is given in Fig. 11. Through the use of a frequency doubler, the output range of the dye laser can be extended to 2100 Å. The output wavelength is selected by a diffraction grating mounted in a drive mechanism, which can be controlled manually or by the Molectron DL-040A Scan Control. The scan control can automatically scan with rates of 1 Å/ min to 1000 Å/ min.

The output power of the laser is monitored using a United Detector Technology Model-80X Opto-Meter. This can measure power down to 10^{-2} μwatt, but the minimum pulse width is 5 msec. Thus, with the use of a recorder, the Opto-Meter is used to measure only relative changes in

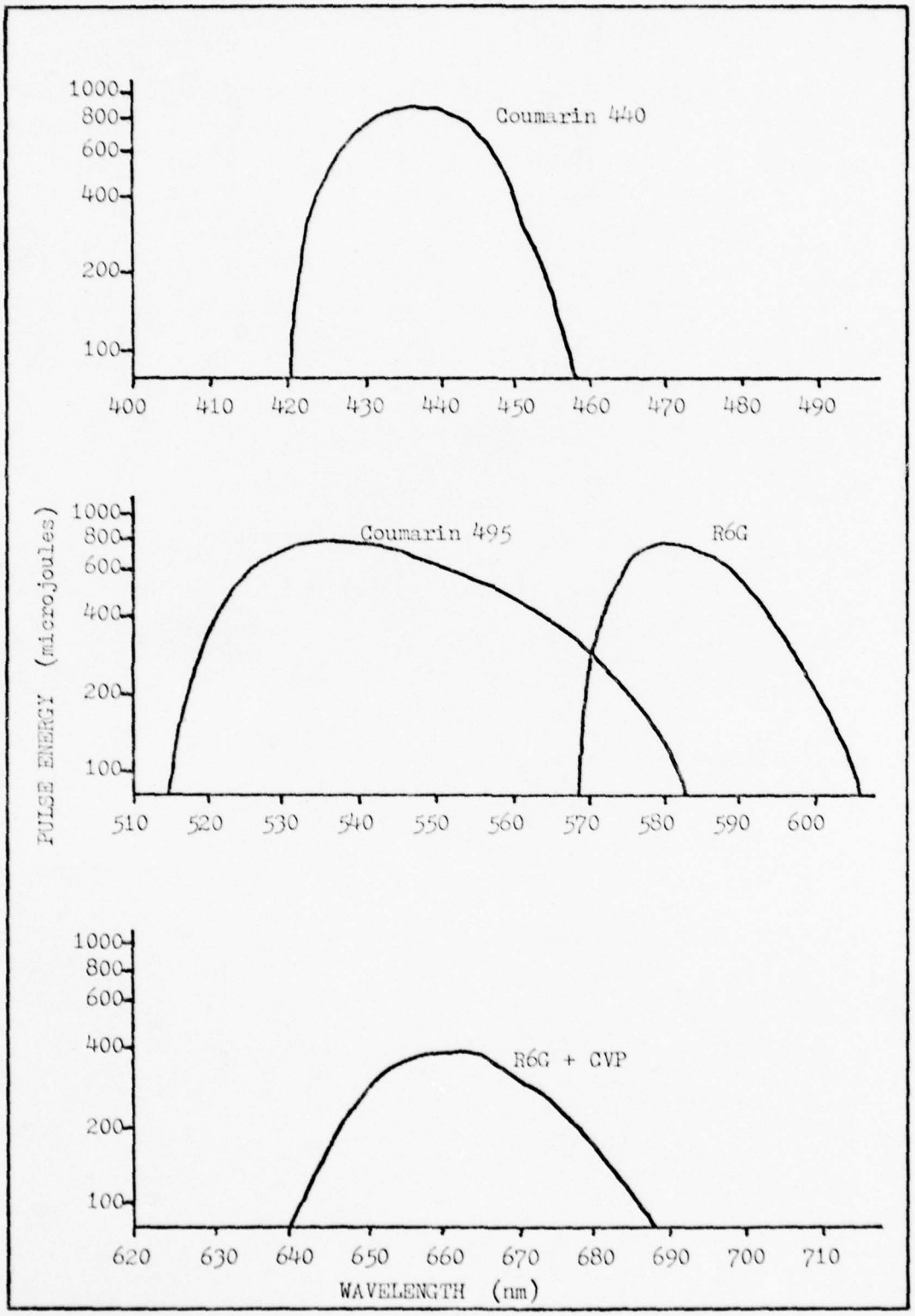

Fig. 11. Dye Laser Pulse Energy

power. A calibrated thermopile is available for accurate power measurements.

Optics

The position of the optical components is shown schematically in Fig. 12. An aperture of 5 mm is located 2.5 cm from the dye laser output port. A Melles Griot pellicle is located 9 cm from the aperture and reflects 50% of the beam to an additional pellicle 76 cm away. The transmitted beam continues 13 cm to the detector head of the Opto-Meter, and the reflected portion is directed to a PIN diode located 30 cm away.

The sample tube is positioned 28 cm from the dye laser. The fluorescence is focused onto the entrance slit of the monochromator by a 2.54 cm diameter lens of focal length 12.7 cm, which is located 25.4 cm from the entrance slit and 25.4 cm from the center of the sample tube. The monochromator is a Jarrell-Ash Mark V Half-Meter Ebert Scanning Spectrometer, which has a 52 mm by 52 mm grating of 1180 grooves/mm and blazed for 4000 Å. The entrance slit is 1 mm wide, and the exit slit is 1.1 mm wide.

Mounted at the exit of the monochromator is an Emitronics 9816B photomultiplier. This has a 14 stage linear dynode chain with an S-20 response covering the range 3000 Å to 8500 Å. The photomultiplier is run at 2000 volts.

Electronics

Several of the electronic components are used for both experimental methods; some are used for only one method. The function of each component can be briefly described. The Ortec Model T105/N Discriminator produces a standard -800 mV signal for each input pulse when that input

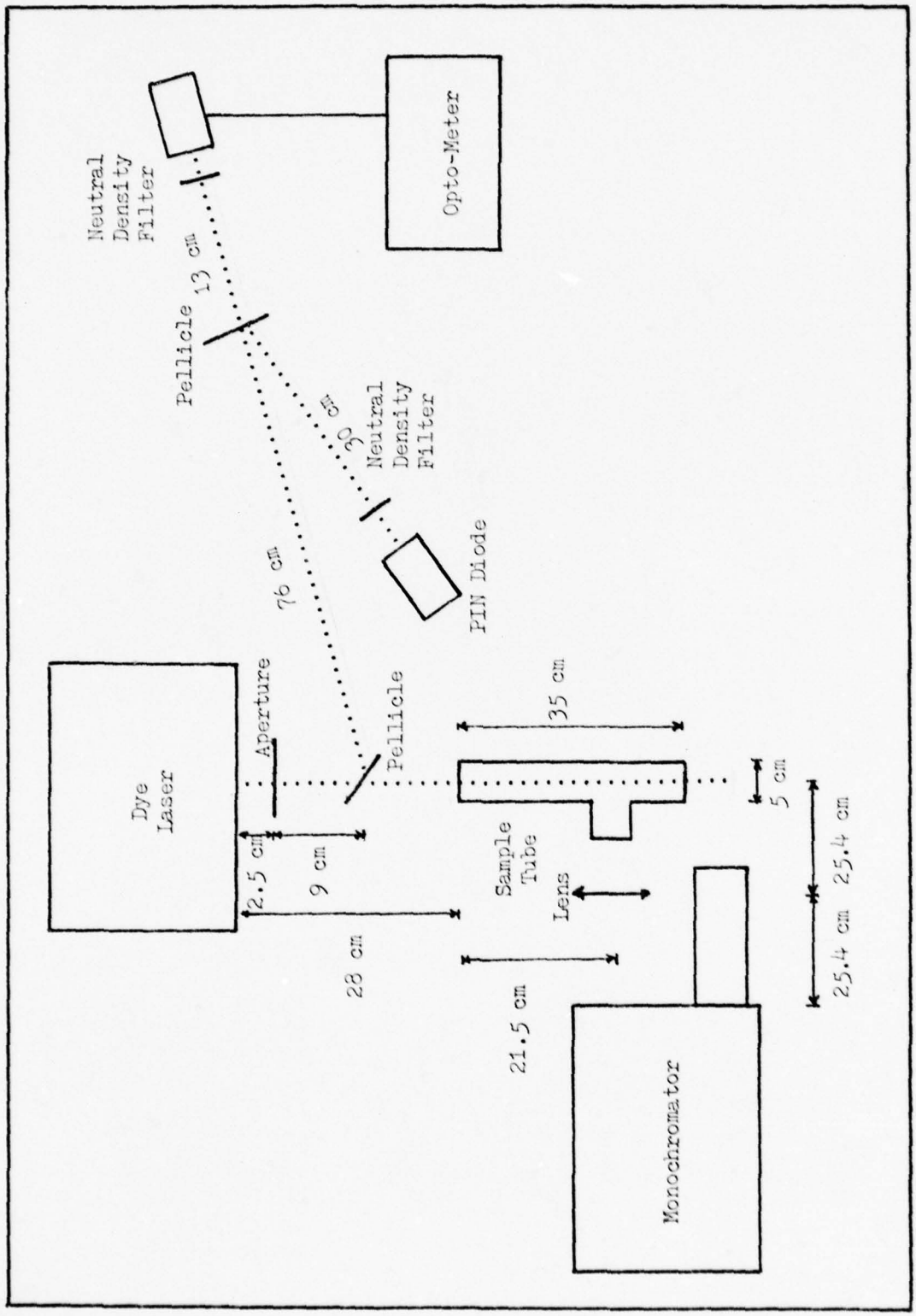

Fig. 12. Schematic of Optics

pulse exceeds a threshold value. This threshold can be varied through the use of a potentiometer, and the width of the output pulse is controlled by a variable external delay line. The discriminator can be operated in either a gated mode, which requires a positive 4 to 12 volt gating signal, or an ungated mode.

The Ortec Model LG105/N Linear Gate and Stretcher integrates an input signal and produces an output signal which has the maximum amplitude held for 3 μsec. The gate and stretcher can be operated in the gated mode, which requires a gating signal of -800 mV, or in the ungated mode. The Fluke Model 1900A Multi-Counter is capable of making frequency and totalize measurements. In the frequency mode, the resolution can be set at 0.1 Hz, 1 Hz, 10 Hz, and 100 Hz. In the totalize mode, the maximum number of counts is 999,999. The multi-counter accepts signals with a minimum pulse width of 20 nsec.

The Ortec Model 447 Time to Pulse Height Converter provides an output pulse with an amplitude that is proportional to the time interval between a Start input and a Stop input; the full range output amplitude is 10 volts. A front-panel switch allows the choice of three ranges: 50 nsec, 250 nsec, and 500 nsec. An output signal is generated only if a Stop signal follows a Start signal within the selected time range. The Start input can be operated in a gated mode, which requires a gating signal of two volts, or the ungated mode. In either mode, the device needs at least 24 nsec after the Start signal to process a Stop signal. If the Stop signal occurs prior to this 24 nsec, a false signal is produced indicating an elapsed time of 24 nsec.

A Hewlett Packard Model 8012B Pulse Generator is used to provide a gating signal to the discriminator. By use of external controls, the

output amplitude can be varied from 0.1 to 10 volts, the pulse width can be varied from 10 nsec to 1 sec, and the pulse delay can be adjusted from 35 nsec to 1 sec.

An Ortec Model DB463 Delay Box is used to delay signals. Four sets of switches can be operated independently or in series. Each set of switches allows delays of 0.5, 1, 2, 4, 8, 16, and 32 nsec. A Tektronics Model 7904 Oscilloscope is used for signal analysis. The oscilloscope includes a camera which uses Polaroid Type 47 film.

A Hewlett Packard Model 5400A Multi-Channel Analyzer (MCA) is used for pulse height analysis. The amplitude of each input pulse determines a memory channel location, which is incremented. After the accumulation of many input pulses, the MCA data shows the number of pulses as a function of pulse amplitude. A total of 1024 memory channels are available, and the maximum input is 10 volts. The output data can be printed on paper tape or displayed on an integral oscilloscope. A camera using Polaroid Type 107 film is available for recording the oscilloscope display.

IV. Procedure

A discussion of the experimental procedure and techniques will be divided into five areas: (1) pumpdown and outgassing, (2) gas handling, (3) dye laser and monochromator, (4) first experimental method, and (5) second experimental method.

Pumpdown and Outgassing

For initial pumpdown of the vacuum system, the Welch mechanical pump is turned on and valves 1, 2, 5, 8, and 9 are opened; all other valves are closed (see Fig. 10). The mechanical pump of the Veeco Leak Detector is turned on and the cold trap is filled with LN_2. The diffusion pump is then turned on. After the mechanical pump has evacuated the system to a pressure of less than one torr, as determined by the thermocouple gauge, valve 8 is closed and the throttle valve of the leak detector is opened.

To promote outgassing of the sample tube, a voltage is applied to the heat tape around the sample tube until the sample tube reaches a temperature greater than 105°C. The pressure is then monitored using the McLeod gauge. Outgassing continues until a pressure of about one millitorr is reached in the sample tube.

Gas Handling

After system pumpdown, valves 1 and 9 are closed, and the throttle valve of the leak detector is closed. A small amount of NO_2 is introduced into the tubing between valves 3 and 4 by slightly opening and then closing valve 4. Valve 3 is opened slightly and then closed; next,

valve 5 is closed. Valve 6 is then opened to freeze out NO_2 until the desired pressure is reached, as determined by the thermocouple gauge. To protect the mercury of the McLeod gauge from NO_2 contamination during this procedure, the McLeod gauge is closed off from the system by a clamp on a small section of rubber tubing. After valve 6 has been closed, the clamp is opened and the pressure equalizes. The McLeod gauge is then used to determine the pressure accurately. Because NO_2 exists as both NO_2 and N_2O_4, the pressure must be accurately measured to determine the degree of dissociation (Ref 3:211-213). After the experiment is completed, the remaining NO_2 is frozen out of the sample tube.

Dye Laser and Monochromator

Once an absorption wavelength of NO_2 has been selected, a laser dye must be chosen that covers that wavelength. This dye is put into the dye laser reservoir, and the dye laser is tuned to the absorption wavelength. The output power of the dye laser is then maximized following the instructions of the equipment manual. The laser power is monitored using the Opto-Meter and recorder.

The monochromator and lens are positioned as shown in Fig. 12; this results in a full-size image at the entrance slit of the monochromator. The monochromator is tuned to the absorption wavelength for resonance fluorescence or to a longer wavelength if the fluorescence of other emission lines is to be monitored.

First Experimental Method

The equipment is connected as shown in Fig. 13. The PIN diode is used to detect the laser pulse and provide a reference time relative to

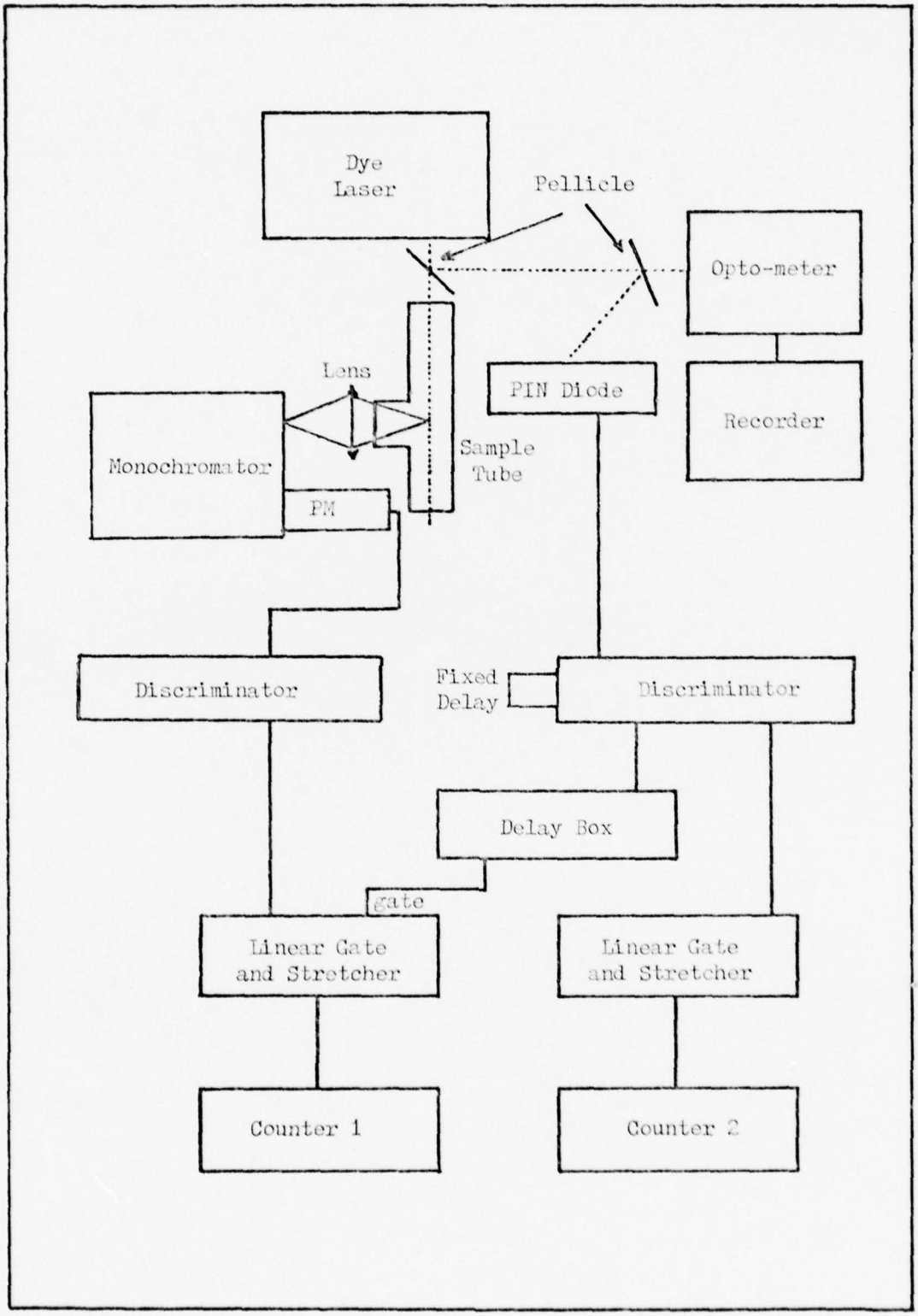

Fig. 13. Schematic of First Experimental Method

that pulse. Neutral density filters are used so that the laser pulse does not overload the PIN diode. To check that the PIN diode is not being overloaded, the output of the PIN diode is checked on the oscilloscope; the signal should have an amplitude of about 150 mV and a pulse width of 30 nsec. The output of the PIN diode is used as the input for one discriminator, which is operated in the ungated mode. This discriminator serves two functions. First, the input threshold is set high enough to eliminate noise. Second, it produces a standard output pulse compatible with the other electronics.

One output of the discriminator is used as the input of a linear gate and stretcher, which is operated in the ungated mode. The linear gate and stretcher output is then used as the input of counter #2. If the linear gate and stretcher were not used, short output pulses of the discriminator might not be detected. An additional output of the discriminator is used to provide a gating signal to a second linear gate and stretcher. The width of the gating interval is determined by a fixed length of delay line attached to the discriminator; this gating interval was shown as τ in Fig. 7.

The output of the photomultiplier is used as the input to a second discriminator, which is operated in the ungated mode. The input threshold of this discriminator is used to eliminate small signal noise. The output of the discriminator is used as the input to the second linear gate and stretcher, which is operated in the gated mode. The gating signal, which was mentioned previously, comes from the first discriminator and goes into a delay box prior to reaching the linear gate and stretcher. This delay box is used to vary the start of the gate interval relative to the laser pulse. A delay of 22 nsec matches the start

of the gating interval with the first photomultiplier pulses of the fluorescence. The output of the second linear gate and stretcher is used as the input to counter #1.

To insure that there is a gate pulse for each laser pulse, the frequency mode of counter #2 is used. The number of pulses per second should be the same as the laser pulse repetition rate. To verify that less than one count is received per laser pulse, the frequency mode of counter #1 is used. If the count is greater than one per laser pulse, neutral density filters are placed at the entrance slit of the monochromator.

To measure the lifetime for the gas sample, the delay box is set to 22 nsec. Both counters are set to the totalize mode. After a fixed number of laser pulses, as determined by the reading of counter #2, the number of photomultiplier counts on counter #1 is recorded. The start of the gate interval is then moved relative to the laser pulse by increasing the delay of the delay box. Both counters are reset, and after the same number of laser pulses, the number of photomultiplier counts on counter #1 is again recorded. This procedure is repeated for additional delay settings of the delay box. The resulting data is exponentially dependent on the fluorescence decay rate as shown by Eq (30).

The lifetime can be determined by the number of counts measured at times t_1 and t_2. For an exponential decay, this lifetime is given by the equation

$$\tau = \frac{t_2 - t_1}{\ln(N_1/N_2)} \tag{49}$$

where N_1 is the number of counts measured at time t_1 and N_2 is the number of counts measured at time t_2. The error in the value of τ is

$$\frac{s_\tau}{\tau} = \sqrt{\frac{s_{t_1}^2 + s_{t_2}^2}{(t_2 - t_1)^2} + \frac{\left[s_{N_2} / N_2\right]^2 + \left[s_{N_1} / N_1\right]^2}{\ln^2(N_2 / N_1)}} \qquad (50)$$

where s_τ = the error in the lifetime τ

s_{t_1} = the error in the measurement of t_1

s_{t_2} = the error in the measurement of t_2

s_{N_1} = the error in the measurement of N_1

s_{N_2} = the error in the measurement of N_2

Second Experimental Method

For the second experimental method, the equipment is connected as shown in Fig. 14. The PIN diode is again used to detect the laser pulse and provide a reference signal relative to that pulse. As in the first method, neutral density filters are used to prevent overloading the PIN diode. The output of the PIN diode is used as the input for one discriminator, which is operated in the ungated mode. One output of the discriminator is used to provide the Start signal for the time to pulse height converter (TPHC). The signal first goes to one line of the delay box, and the output of the delay box goes to the Start input of the TPHC. The delay box can then be used to vary the Start signal relative to the laser pulse. An additional output of the discriminator is used to provide a trigger signal for the pulse generator. The pulse generator then provides a gating signal for a second discriminator.

The output of the photomultiplier is used as the input to the second discriminator, which is operated in the gated mode. One output of the discriminator is used as the input to a linear gate and stretcher, which is operated in the ungated mode. The output of this linear gate

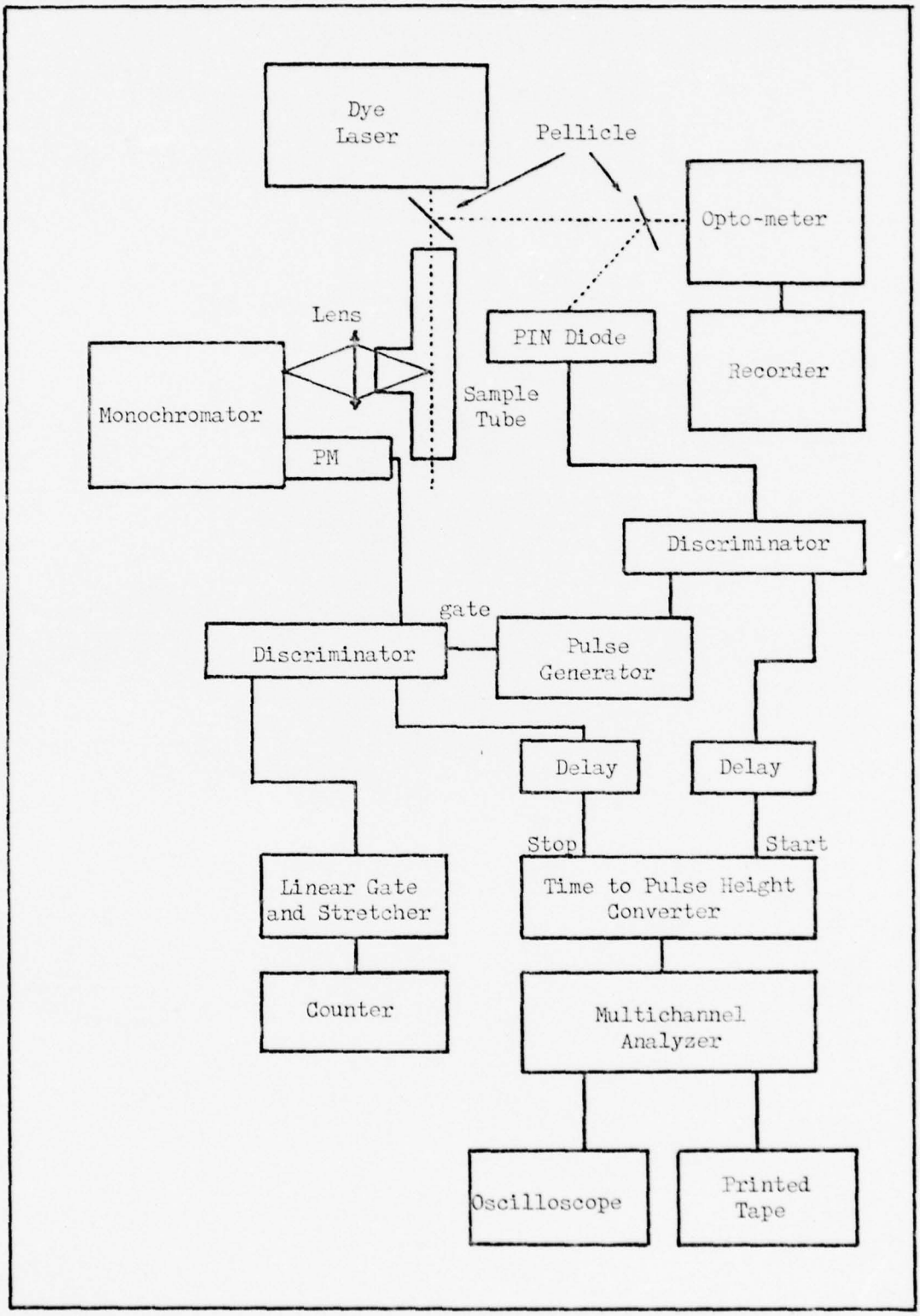

Fig. 14. Schematic of Second Experimental Method

and stretcher then goes to a counter. This counter is used to determine the number of photomultiplier counts per laser pulse which come during the gating interval. Another output of the second discriminator is used to provide Stop signals for the TPHC. The signal first goes to the second line of the delay box and the output of the delay box goes to the Stop input of the TPHC. The delay box can then be used to vary the Stop signal relative to the laser pulse. The output of the TPHC is used as the input of the multichannel analyzer (MCA).

To measure the fluorescence lifetime of the gas sample, one of the three ranges of the TPHC is selected. The gate interval determined by the width of the gating signal from the pulse generator is then set to at least the range selected on the TPHC. The start of the gate interval is set by changing the delay in the pulse generator relative to the laser pulse. The start of the gate interval can be set at a time after scattering occurs; thus, these unwanted photomultiplier signals can be eliminated when measuring resonance fluorescence. Additionally, if the start of the gate interval is set to 24 nsec after the Start signal to the TPHC, the 24 nsec dead time of the TPHC can be avoided. Since the delay in the pulse generator is set by a vernier control, refined adjustments to the start of the gate interval can be made by changing the delay of the Start and Stop signals. For example, an addition of 5 nsec to the delays of both the Start and the Stop signals is the same as changing the start of the gate interval 5 nsec earlier relative to the laser pulse.

Since the full range output of the TPHC is 10 volts, the input range of the MCA is set to 10 volts. Prior to data taking, the memory channels of the MCA are erased. The MCA is then set to accumulate TPHC

signals until enough data is stored in the channels to produce a statistical curve. After data accumulation, the data in the MCA can be viewed on the integral oscilloscope or printed on paper tape. Since each memory channel corresponds to a point in time relative to the laser pulse, the lifetime of the exponential curve can be calculated using Eq (49).

V. Results and Discussion

Both experimental methods to measure fluorescence lifetimes were tested during this thesis effort, and many problems were eliminated. General results common to both experimental methods are presented in this chapter, followed by a discussion of the results for each experimental method.

General Results

The dye laser and N_2 laser operated satisfactorily. Four dyes--R6G, R6G + CVP, Coumarin 495, and Coumarin 440--were used during the course of the experiment and covered approximately the range of wavelengths as shown in Fig. 11. The output power of the dyes was less than that specified in the dye laser manual. For example, the output power of Coumarin 440 was 1.3 mwatt when pulsed at 10 pulses per second at 4304 Å; output power on the order of 5 mwatt was expected. The width of the dye laser pulse was less than 10 nsec, as shown in the photograph of the PIN diode signal (Fig. 15).

The scan control, which turns the grating within the dye laser to select the output wavelength, was very reliable in scanning at constant speeds. This was necessary when absorption measurements were taken. A sample absorption measurement for 30 torr of NO_2 is shown in Fig. 16, where R6G was scanned over the wavelength range 5780 Å to 5789 Å. This measurement was taken by scanning the dye laser over a frequency range and recording the laser intensity after passing through the empty sample tube; the scan was then repeated with NO_2 in the sample cell. The

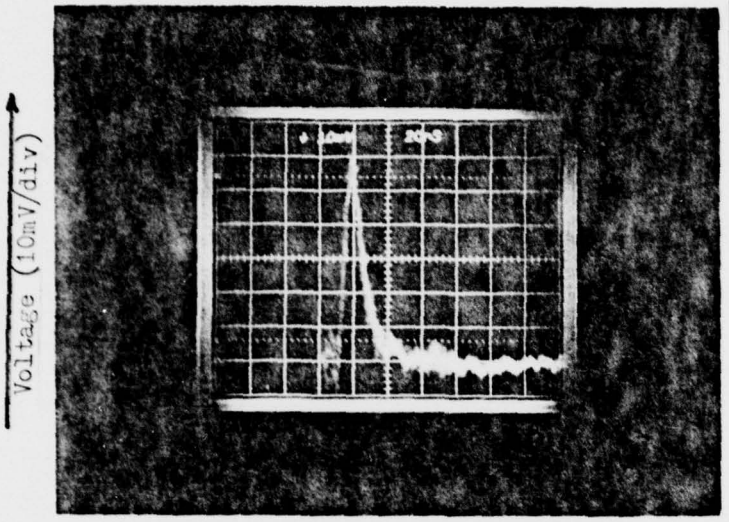

Fig. 15. PIN Diode Signal

periodic variation in the output intensity of the laser beam is due to an interference effect within the dye laser; possibly the output window. Because an etalon was not used in the dye laser, it was not possible to identify individual absorption bands. A neutral density filter placed in front of the dye laser beam verified that saturation of the gas sample was not taking place.

The gas handling system was satisfactory in delivering and evacuating NO_2 to and from the sample tube. Pressures from 1 mtorr to 30 torr were maintained in the sample tube; however, difficulty was encountered in accurately measuring these pressures. A McLeod gauge was used for accurate pressure measurements, but contact with the NO_2 contaminated the mercury of the gauge. After continued use, this interfered with the use of the gauge, and the mercury had to be replaced.

The output signals of each of the pieces of electronics were checked on the oscilloscope. With three exceptions, all of the electronics

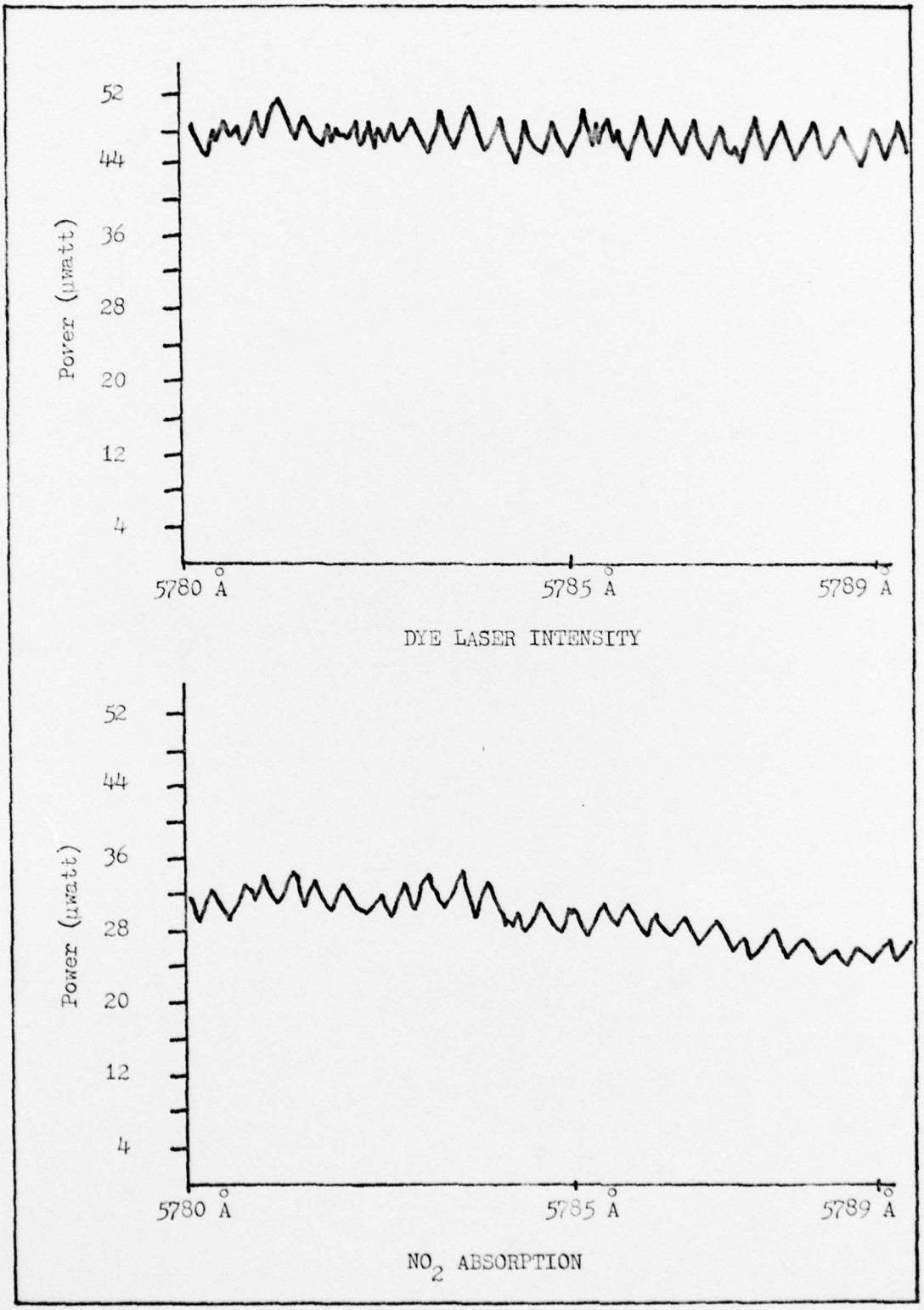

Fig. 16. NO_2 Absorption (30 torr)

operated satisfactorily. The time to pulse height converter did not put out a maximum voltage of 10 volts. For the 250 nsec scale, the 250 nsec output was 9.1 volts. However, a plot of output voltage versus time was linear, and the device could be used to measure elapsed time. The MCA developed a problem during the course of the experiment; it would not accumulate data in every eighth channel. An electronic circuit board must be replaced within the MCA to correct this problem, but this board was not available. Finally, the photomultiplier displayed ringing, which is a sign of an impedance mismatch. A photograph of the photomultiplier ringing is shown in Fig. 17. All attempts to locate the source of this ringing were unsuccessful; a possible location is the socket of the photomultiplier tube. The background count of the photomultiplier tube during the 10 μsec gating interval averaged 0.011 counts per laser pulse. For resonance fluorescence, scattering from the ends of the sample tube increased this background count average to 0.017 counts per laser pulse. A major problem eliminated during the course

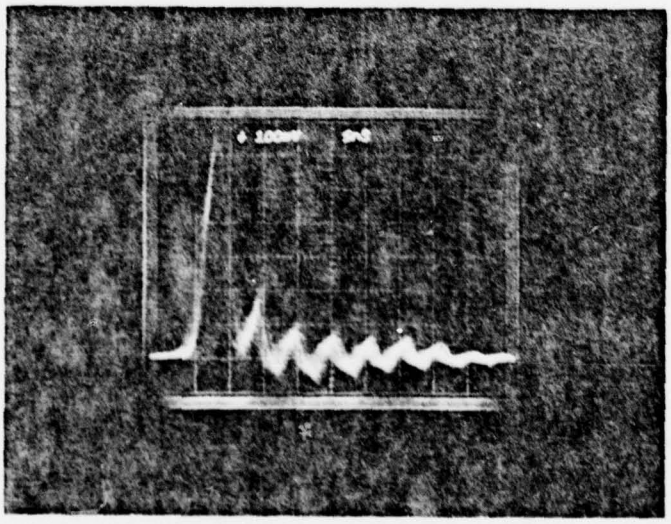

Fig. 17. Photomultiplier Ringing

of the experiment was additional scattering from the entrance and exit ports of the insulative box surrounding the sample tube. Considerable data was taken of this scattering, which initially was thought to be the fluorescence signal. This scattering was eliminated by painting the interior of the insulative box black and by positioning the box so that the laser beam travelled through the center of the entrance and exit ports.

Various fluorescence lines of NO_2 were observed. Resonance fluorescence was examined at 6512 Å, 5792 Å, 5461 Å, 4480 Å, 4448 Å, 4390 Å, 4350 Å, and 4304 Å. Non-resonance fluorescence at 4740 Å and 4545 Å was also examined. The strongest fluorescence signal was observed at 4740 Å when exciting at 4304 Å; however, this signal was still quite weak.

First Experimental Method

The first experimental method was tested when it was not known that scattering from the insulative box dominated the fluorescence signal. However, the system was checked and found to operate satisfactorily. Operation of the gating system was verified by connecting the photomultiplier output directly to the linear gate and not through a discriminator. Because of the photomultiplier ringing, false counts were registered beyond the original counts. This resulted in an artificial decay measurement, and using the first experimental method, it was possible to measure a 13 nsec lifetime for this false decay. Although this was not a measure of fluorescence decay, it demonstrated that the method can be used to measure decay times on the order of 10 nsec.

The length of time it took to accumulate data was a disadvantage to this method. During the measurement time, the declining power of the laser allowed a decrease in the excited state population density at the

end of each laser pulse. Thus, the laser power had to be monitored, and the decay measurements were normalized to a standard power level. The use of fresh dyes in the dye laser minimized this power decline. A rise in the room temperature was also observed to cause a decline in the dye laser power.

Second Experimental Method

The second experimental method was used to measure the lifetime for NO_2 at 4740 Å. A photograph of the decay curve for one torr is shown in Fig. 18, and a plot of the data appears in Fig. 19. The 500 nsec range of the TPHC was used for this measurement, which was taken at room temperature. Using Eq (49), this data yielded a lifetime of 150 ± 16 nsec. The primary error in this number is due to the low number of counts taken. It is not known whether Eq (20), Eq (24), or Eq (25) applies to this non-resonance fluorescence.

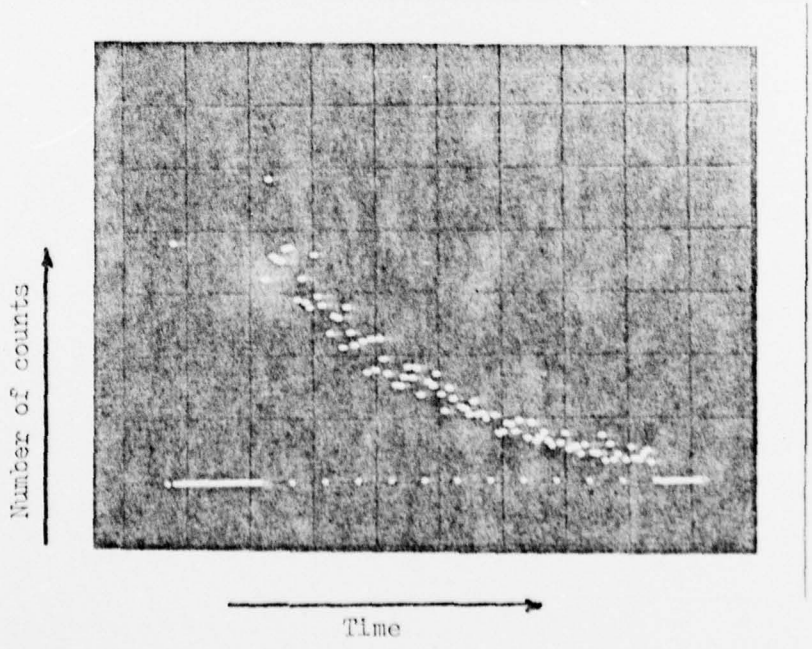

Fig. 18. MCA Photograph of Fluorescence Decay

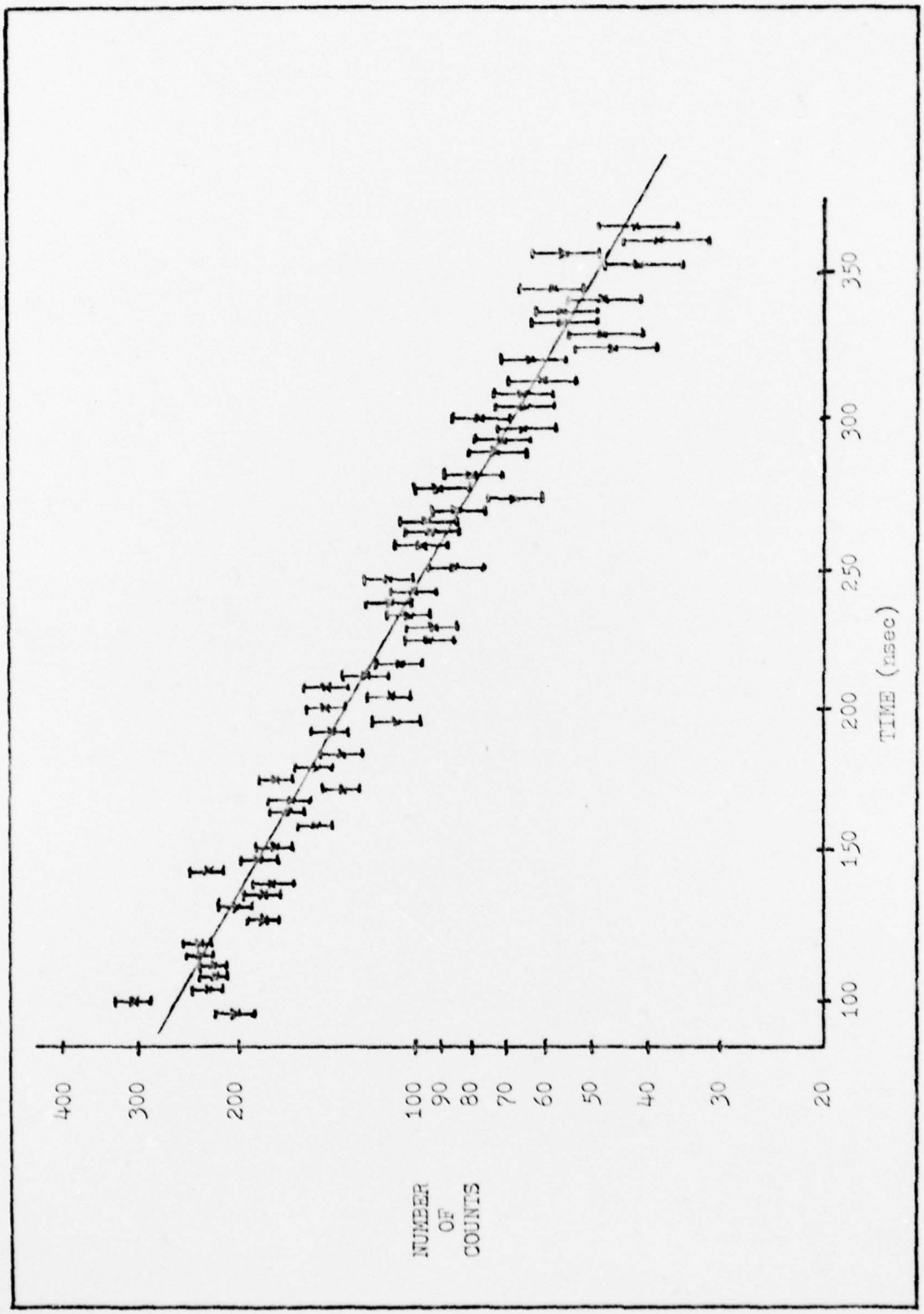

Fig. 19. NO_2 Fluorescence Decay (1 torr)

To show that this method is capable of measuring lifetimes on the order of 10 nsec, the scattered light from the entrance and exit ports of the insulative box was examined. Two pulses were clearly detected, as shown in the MCA photograph of Fig. 20. The width of each pulse is 6 nsec, which is the approximate width of the laser pulse. Thus, the second experimental method is also capable of measuring the short lifetimes expected in combustion flames.

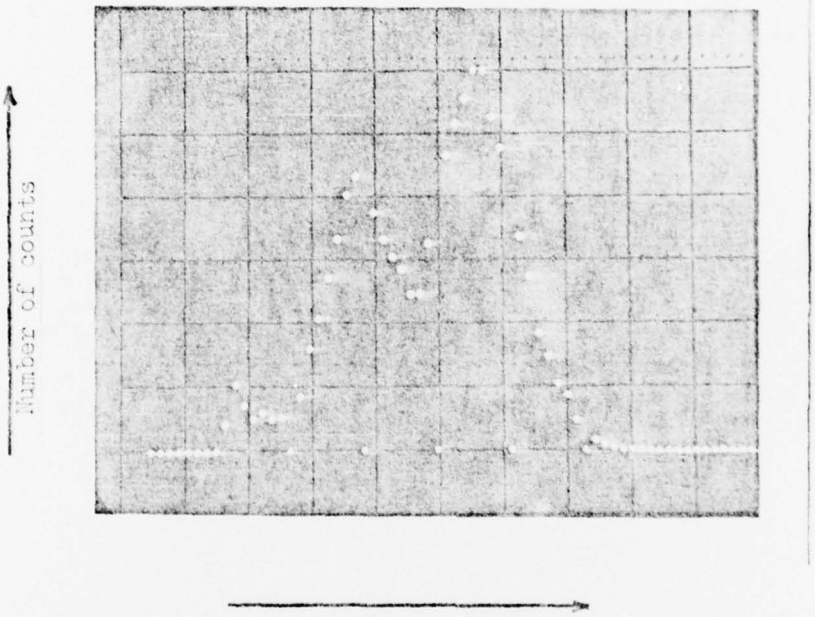

Fig. 20. MCA Photograph of Scattered Light Data

VI. Conclusions and Recommendations

Conclusions

During this thesis effort, two experimental methods for measuring fluorescence lifetimes were investigated. Based upon this work, several conclusions can be made:

1. Both experimental methods can be used to measure fluorescence lifetimes as short as 10 nsec.

2. The second experimental method can accumulate data in a shorter period of time than the first experimental method. Such a consideration may be important if the temperature or pressure of the gas sample is changing.

3. A stronger fluorescence signal would improve the photon counting rate and reduce the statistical error of the calculated lifetime. No reason could be determined for a measured fluorescence signal smaller than that expected by calculations based on the absorption coefficient.

4. Insufficient data was taken to determine which transitions were involved for the fluorescence wavelengths observed.

Recommendations

Based upon the results of this study, the following recommendations are made:

1. The vacuum system should be improved to better control the pressure of the gas sample.

2. The pressure of the gas sample should be measured using a baratron instead of a McLeod gauge. This would eliminate the problem of NO_2 contamination of the mercury of the McLeod gauge.

3. Because photomultiplier ringing could not be eliminated, either the photomultiplier socket should be replaced or another photomultiplier tube should be used.

4. Measurements should be taken of fluorescence lifetimes of NO_2 at different pressures. The effect of collisions on quenching could then be determined.

5. A time to pulse height converter with a range longer than 500 nsec should be used for measurements of NO_2 lifetimes.

6. The quenching effects of additional species on NO_2 lifetimes should be investigated since several species would be present in an actual combustion flame.

7. A frequency doubler for the dye laser should be obtained in order to look at other regions of the NO_2 emission spectrum or the emission spectrum of other species. However, since the use of a doubler reduces the intensity of the dye laser beam, the fluorescence signal of NO_2 may be too weak to detect.

8. The strength of the fluorescence signal should be increased. The use of an uncoated pellicle would increase the intensity of the laser beam going through the sample tube. The image of the fluorescence region, which is parallel to the laser beam, can be rotated to fill the entrance slit of the monochromator. The laser beam can be focused in the region which is viewed by the entrance slit; the width of the entrance slit can be optimized for signal intensity and resolution. The strength of the fluorescence signal could also be increased by using a monochromator with a smaller f-number, a mirror behind the sample tube, and broad band anti-reflective coatings.

Bibliography

1. Banwell, C. N. Fundamentals of Molecular Spectroscopy (Second Edition). London: McGraw-Hill Book Co., 1972.

2. Cobine, James D. Gaseous Conductors: Theory and Engineering Applications. New York: Dover Publications, Inc., 1958.

3. Daniels, Farrington and Robert A. Alberty. Physical Chemistry (Third Edition). New York: John Wiley & Sons, Inc., 1966.

4. Donnelly, V. M. and F. Kaufman. "Fluorescence Lifetime Studies of NO_2. I. Excitation of the Perturbed $^2B_2$ State Near 600 nm." Journal of Chemical Physics, 66: 4100-4110 (May 1977).

5. Douglas, A. E. "Anomalously Long Radiative Lifetimes of Molecular Excited States." Journal of Chemical Physics, 45: 1007-1015 (February 1966).

6. Eckbreth, A. C., et al. Review of Laser Raman and Fluorescence Techniques for Practical Combustion Diagnostics. EPA-600/7-77-066. U. S. Environmental Protection Agency, Office of Research and Development, Washington, D.C. 20460, June 1977.

7. Gillispie, Gregory D. and Ahsan U. Khan. "The Electronic Structure of NO_2. II. The $A^2B_2 \leftarrow X^2A_1$ and $B^2B_1 \leftarrow X^2A_1$ Absorption Systems." Journal of Chemical Physics, 65: 1624-1633 (September 1976).

8. Gillispie, Gregory D., et al. "The Electronic Structure of Nitrogen Dioxide. I. Multiconfiguration Self-consistent-field Calculation of the Low-lying Electronic States." Journal of Chemical Physics, 63: 3425-3444 (October 1975).

9. Herzberg, Gerhard. Molecular Spectra and Molecular Structure. Vol. III: Electronic Spectra and Electronic Structure of Polyatomic Molecules. Princeton, New Jersey: D. Van Nostrand Company, Inc., 1967.

10. Jackels, Charles F. and Ernest R. Davidson. "The Two Lowest Energy $^2A'$ States of NO_2." Journal of Chemical Physics, 64: 2908-2917 (April 1976).

11. -----. "An Ab Initio Potential-energy Surface Study of Several Electronic States of NO_2." Journal of Chemical Physics, 65: 2941-2957 (October 1976).

12. Keyser, L. F., et al. "Radiative Lifetime and Collisional Quenching of NO_2 Fluorescence and Nature of the Air Afterglow." Chemical Physics Letters, 2: 523-525 (December 1968).

13. Neuberger, Dan and A. B. F. Duncan. "Fluorescence of Nitrogen Dioxide." Journal of Chemical Physics, 22: 1693-1696 (January 1954).

14. Pearse, R. W. B. and A. G. Gaydon. The Identification of Molecular Spectra (Third Edition). New York: John Wiley & Sons Inc., 1963.

15. Piepmeier, E. H. "Theory of Laser Saturated Atomic Resonance Fluorescence." Spectrochimica Acta, 27B: 431-443 (1972).

16. Price, William J. Nuclear Radiation Detection. New York: McGraw-Hill Book Co., 1958.

17. Schafer, F. P. Dye Lasers. New York: Springer-Verlag, 1973.

18. Smalley, Richard E., Lennard Wharton, and Donald H. Levy. "The Fluorescence Excitation Spectrum of Rotationally Cooled NO_2." Journal of Chemical Physics, 63: 4977-4989 (August 1975).

19. Stevens, Charles G. and Richard N. Zare. "Rotational Analysis of the 5933 A Band of NO_2." Journal of Molecular Spectroscopy, 56: 167-187 (1975).

20. Tucker, A. W., et al. "Atmospheric NO_2 Determination by 442-nm Laser Induced Fluorescence." Applied Optics, 14: 1418-1422 (June 1975).

21. Uselman, William M. and Edward K. C. Lee. "A Study of Electronically Excited Nitrogen Dioxide in its First Predissociation Region: Fluorescence Emission, Lifetimes, and Electronic Quenching." Journal of Chemical Physics, 64: 3457-3462 (April 1976).

VITA

John James Wharton, Jr. was born on 28 May 1949 in Warrensburg, Missouri. He is the son of Mr. and Mrs. Jack Wharton. He attended the University of Missouri at Columbia, Missouri, after graduating from high school in 1967. In 1971 he received the degree of Bachelor of Science in Electrical Engineering and a commission in the United States Air Force. After receiving training as a Missile Launch Officer at Vandenberg Air Force Base, California, he was assigned to the 44th Strategic Missile Wing (SAC), Ellsworth Air Force Base, South Dakota. Captain Wharton began his tour at the Air Force Institute of Technology in June 1976.

Permanent address: 1601 South Market St.
Holden, Missouri 64040

Unclassified

SECURITY CLASSIFICATION OF THIS PAGE *(When Data Entered)*

REPORT DOCUMENTATION PAGE		READ INSTRUCTIONS BEFORE COMPLETING FORM
1. REPORT NUMBER GEP/PH/77-16	2. GOVT ACCESSION NO.	3. RECIPIENT'S CATALOG NUMBER
4. TITLE *(and Subtitle)* LIFETIME MEASUREMENTS USING FLUORESCENCE EMISSION		5. TYPE OF REPORT & PERIOD COVERED MS Thesis 6. PERFORMING ORG. REPORT NUMBER
7. AUTHOR(s) John J. Wharton Jr. Captain		8. CONTRACT OR GRANT NUMBER(s)
9. PERFORMING ORGANIZATION NAME AND ADDRESS Air Force Institute of Technology (AFIT-EN) Wright-Patterson AFB, Ohio 45433		10. PROGRAM ELEMENT, PROJECT, TASK AREA & WORK UNIT NUMBERS
11. CONTROLLING OFFICE NAME AND ADDRESS		12. REPORT DATE December 1977 13. NUMBER OF PAGES 62
14. MONITORING AGENCY NAME & ADDRESS*(if different from Controlling Office)*		15. SECURITY CLASS. *(of this report)* Unclassified 15a. DECLASSIFICATION/DOWNGRADING SCHEDULE

16. DISTRIBUTION STATEMENT *(of this Report)*

Approved for public release; distribution unlimited

17. DISTRIBUTION STATEMENT *(of the abstract entered in Block 20, if different from Report)*

18. SUPPLEMENTARY NOTES

Approved for public release; IAWAFR 190-17

JERRAL F. GUESS, Captain, USAF
Director of Information

19. KEY WORDS *(Continue on reverse side if necessary and identify by block number)*

Fluorescence
Lifetime
Nitrogen Dioxide

20. ABSTRACT *(Continue on reverse side if necessary and identify by block number)*

Two experimental methods are developed for measuring fluorescence lifetimes on the order of ten nanoseconds. These data are necessary for measurements of species concentrations in combustion flames. The first method is based on counting photons within a fixed time interval, the position of which can be varied with respect to the excitation time of the sample. The second method uses a time to pulse height converter to measure the elapsed time between excitation of the sample and emission of a photon. The number of photons detected per laser pulse is reduced to one or less in order to obtain a valid

DD FORM 1 JAN 73 1473 EDITION OF 1 NOV 65 IS OBSOLETE

Unclassified

SECURITY CLASSIFICATION OF THIS PAGE *(When Data Entered)*

statistical distribution. A tunable dye laser is used as the excitation source, and nitrogen dioxide is used as the test sample at pressures of 30 torr or less.